

Square planar-tetrahedral interconversion without spin flip in (β -diiminate)Rh(1,3-diene) complexes

Rebecca S. Sherbo,[†] Gurmeet Singh Bindra, Peter H.M. Budzelaar*

Department of Chemistry, University of Manitoba, Winnipeg, MB R3T 2N2, Canada

[†] Present address: Department of Chemistry, The University of British Columbia, 2036 Main Mall, Vancouver, BC V6H 1Z1, Canada

Supporting Information

Contents

Crystal structures.....	3
(^{Et} BDI)Li(THF).....	4
(^{Et} BDI)Rh(COD).....	6
(^{Et} BDI)Rh(PD).....	7
(^{Me} BDI)Ir(BD)	8
Singlet and triplet geometries.....	9
Comparison of calculated and observed NMR parameters	10
Complex 1.....	10
Complex 2a.....	11
Complex 2b.....	11
Complex 3 ^a	12
Complex 4 ^a	12
Complex 5.....	12
(EtBDI)Rh(1,3-CHD) ^d	13
NMR spectra for (^{Et} BDI)Rh(trans-1,3-HD).....	14
Simulation of VT-NMR spectra, (^{Et} BDI)Rh(trans-1,3-HD), imine methyl region.....	22
Eyring plot	25
Fit results:	25
NMR spectra for (^{Et} BDI)Rh(trans/cis-1,3-PD).....	26
Simulation of VT-NMR spectra, (^{Et} BDI)Rh(trans/cis-1,3-PD), imine methyl region.....	32
Eyring plot for <i>trans</i> isomer.....	36
Fit results:	36
Eyring plot for <i>cis</i> isomer	37
Fit results:	37
NMR spectra for (^{Me} BDI)Rh(BD).....	38
Simulation of VT-NMR spectra, (^{Me} BDI)Rh(BD), aryl methyl region.....	40
Eyring plot	40
Fit results:	40
NMR spectra for (^{Me} BDI)Ir(BD).....	41
Simulation of VT-NMR spectra, (^{Me} BDI)Ir(BD), aryl methyl region.....	43
Eyring plot	43
Fit results:	43
NMR spectra for (^{Et} BDI)Rh(2-TMSO-1,3-CHD)	44
Simulation of VT-NMR spectra, (^{Et} BDI)Rh(2-TMSO-1,3-CHD), imine methyl region.	49
Eyring plot	53
Fit results:	53
Calculated b-p energies	54
Calculated TPSSh energies	55

Crystal structures

Table S1. Details of crystal structure determinations.

Complex	(^{Et} BDI)Li(THF)	(^{Et} BDI)Rh(COD)	(^{Et} BDI)Rh (Me ₃ SiO-CHD)	(^{Et} BDI)Rh(PD)	(^{Me} BDI)Rh(BD)	(^{Me} BDI)Ir(BD)
Formula	C ₂₉ H ₃₈ LiN ₂ O	C ₃₃ H ₄₅ N ₂ Rh	C ₃₄ H ₄₉ N ₂ ORhSi	C ₃₀ H ₄₁ N ₂ Rh	C ₂₅ H ₃₁ N ₂ Rh	C ₂₅ H ₃₁ N ₂ Ir
Mol wt	437.55	572.62	632.75	532.56	462.43	551.72
T (K)	293(2)	293(2)	293(2)	293(2)	293(2)	123(2)
Crystal system	Monoclinic	Tetragonal	Triclinic	Monoclinic	Monoclinic	Monoclinic
Space group	C ₂ /c	P ₄ 3 ₂ 12	P-1	P ₂ / ₁ c	P ₂ / ₁ n	P ₂ / ₁ n
a / Å	13.952(8)	9.780(3)	9.744(5)	13.858(4)	13.477(3)	13.5679(2)
b / Å	14.900(8)	9.780(3)	11.613(5)	9.515(4)	13.562(3)	13.3427(2)
c / Å	14.031(10)	30.773(9)	15.834(7)	20.971(7)	13.754(4)	13.5761(2)
α/ deg	90	90	93.135(5)	90	90	90
β/ deg	101.583(6)	90	101.617(15)	98.383(8)	114.866(17)	115.5604(5)
γ/ deg	90	90	104.610(9)	90	90	90
V / Å ³	2857(3)	2943.3(12)	1687.6(14)	2735.7(17)	2280.9(10)	2217.18(6)
Z	4	4	2	4	4	4
D _c / g cm ⁻³	1.017	1.292	1.245	1.293	1.347	1.653
abs coef / mm ⁻¹	0.06	0.603	0.568	0.643	0.760	6.04
F ₀₀₀	948	1208	668	1120	960	1088
index ranges	-16 < h < 16 -18 < k < 18 -16 < l < 16	-11 < h < 11 -11 < k < 11 -37 < l < 37	-11 < h < 11 -14 < k < 14 -19 < l < 19	-16 < h < 16 -11 < k < 11 -25 < l < 25	-16 < h < 16 -16 < k < 16 -16 < l < 16	-16 < h < 16 -16 < k < 16 -16 < l < 16
2θ _{max} / deg	51.0	51.0	51.0	51.0	51.0	51.0
# rflctns	10397	21811	12540	19731	16595	56313
# unique	2663	2741	6275	5102	4250	4126
# > 2σ	1960	2725	6013	4816	3892	3698
GOF	1.192	0.885	1.064	1.059	1.111	1.364
# parameters	152	167	361	293	259	259
R (F _o > 4 σ(F))	0.0779	0.0245	0.031	0.0745	0.0250	0.0201
R (all data)	0.0944	0.0246	0.0322	0.0763	0.0280	0.0271
wR ₂ (all data)	0.2777	0.0681	0.0877	0.1966	0.1966	0.0725
largest peak, hole / e Å ⁻³	0.442, -0.303	0.282, -0.553	0.751, -0.518	4.159, -0.826	0.652 -0.427	1.549 -1.000

$(^{Et}BDI)Li(THF)$

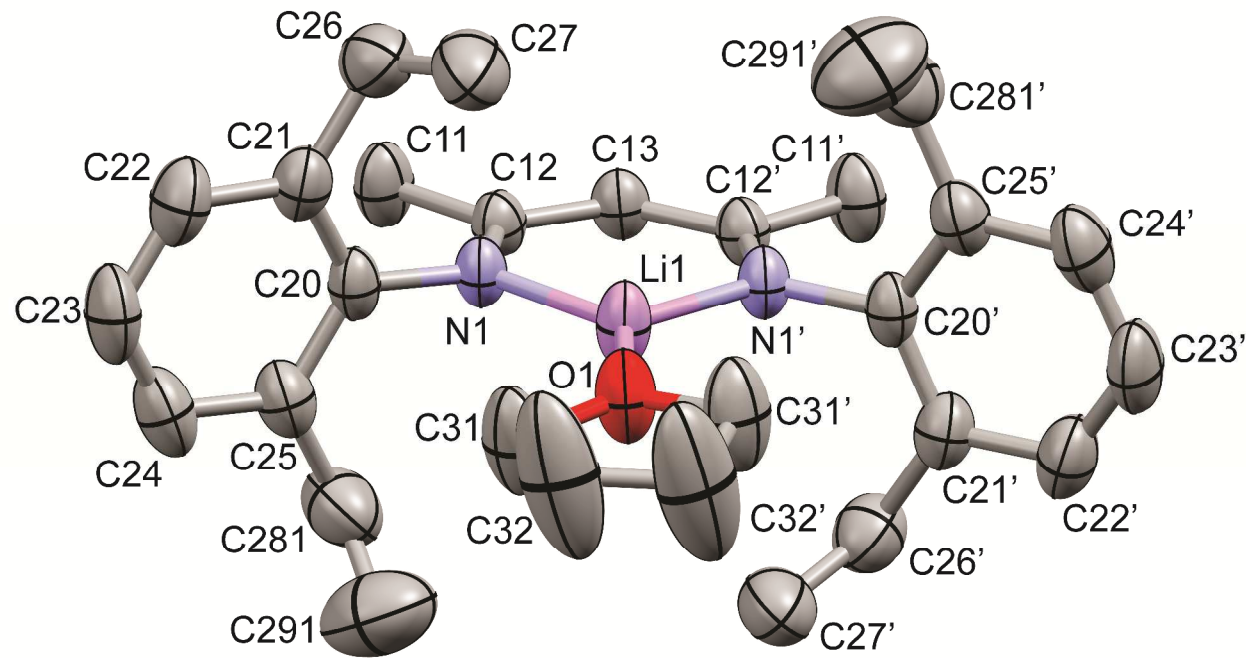


Figure S1. Crystal structure of $(^{Et}BDI)Li(THF)$ (35% probability ellipsoids). Hydrogen atoms omitted for clarity. Only one of the two orientations of the disordered C28-C29 Et group is shown. The molecule is located on a twofold rotation axis.

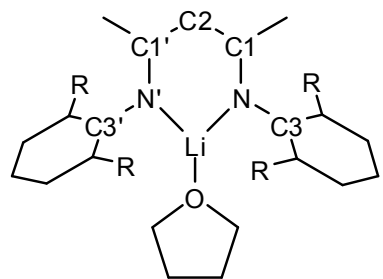


Table S2. Comparison of bond lengths (Å) in (^RBDI)Li(THF) complexes.

	(^{Me} BDI)Li(THF) ^a	(^{Et} BDI)Li(THF) ^b	(^{iPr} BDI)Li(THF) ^c	(^{iPr} BDI)Li(THF) ^d
Li-O	1.862(7)	1.887(6)	1.790(7)	1.889
Li-N	1.912(7), 1.905(9)	1.908(4)	1.957(5)	1.892
N-C1	1.323(5), 1.315(5)	1.318(3)	1.325(3)	1.326(3)
C1-C2	1.405(6), 1.413(5)	1.403(3)	1.410(2)	1.399
N-Li-N'	101.1(3)	100.7(3)	95.5(3)	99.9
Li-N-C3	120.5(3) 120.7(3)	119.4(2)	119.8(2)	118.3
C1-N-C3	119.2(3), 120.7(3)	119.7(2)	119.8(2)	119.5

^a Yao, Y.; Zhang, Z.; Shen, Q.; Sun, J., *Chem. Res. Appln.* **2003**, *15*, 859 (CCDC code KODQAW). Crystallographically independent bond lengths listed separately. ^b this work. ^c Stender, M.; Wright, R. J.; Eichler, B. E.; Prust, J.; Olmstead, M. M.; Roesky, H. W.; Power, P. P., *J. Chem. Soc., Dalton Trans.* **2001**, 3465-3469 (CCDC code CACKIB). ^d Monillas, W.H.; Theopold, K.H.; Yap, G.P.A., *Private Communication to CCDC*, **2007** (CCDC code CACKIB01).

(^{Et}BDI)Rh(COD)

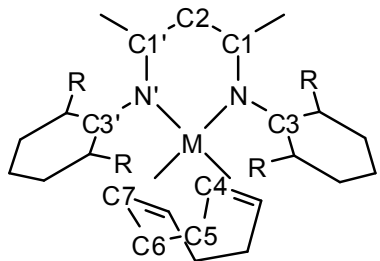


Table S3. Comparison of bond lengths (Å) in (^RBDI)(Rh/Ir)(COD) complexes.

	(^{Mc} BDI)Rh(COD) ^a	(^{Et} BDI)Rh(COD) ^b	(^{iPr} BDI)Ir(COD) ^c
M-(C=C)	2.043	2.045	2.009 2.021
M-N	2.095(2)	2.101(2)	2.096(2) 2.088(2)
N-C1	1.333(2)	1.331(3)	1.352(3) 1.339(3)
C1-C2	1.388	1.384(3)	1.384(5) 1.392(5)
N-M-N'	89.21	89.2(1)	90.1(1)
M-N-C3	119.8	119.3(2)	120.2(2) 120.2(2)
C1-N-C3	114.2	114.9(2)	114.2(2) 114.0(3)
C4-C5-C6-C7	32.0(3)	33.6(4)	28.5(4) 33.0(4)

^a Budzelaar, P. H. M.; Moonen, N. N. P.; de Gelder, R.; Smits, J. M. M.; Gall, A. W., *Eur. J. Inorg. Chem.* **2000**, 753-769 (CCDC code FOPWEM). ^b this work. ^c Bernskoetter, W. H.; Lobkovsky, E.; Chirik, P. J., *Organometallics* **2005**, 24, 6250-6259 (CCDC code DEBCAP). Crystallographically independent bond lengths listed separately.

(^{Et}BDI)Rh(PD)

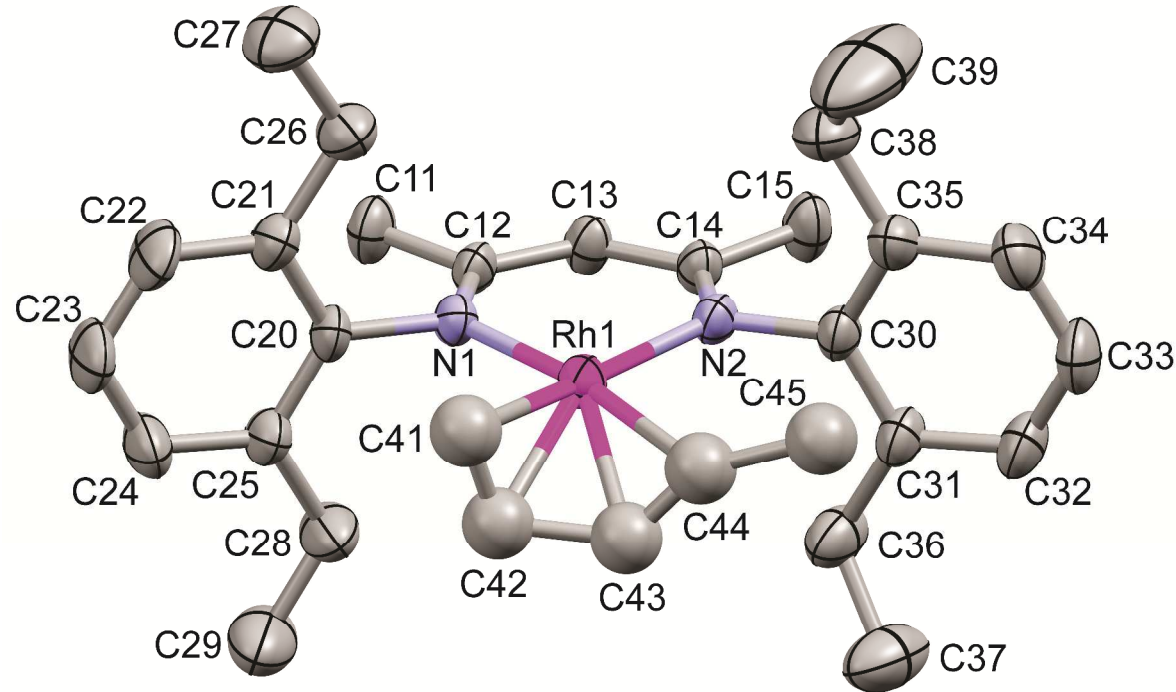


Figure S2. Crystal structure of (^{Et}BDI)Rh(PD) (35% probability ellipsoids). Hydrogen atoms omitted for clarity. Only one of the two orientations of the disordered PD fragment group (refined isotropically) is shown.

$(^{Me}BDI)Ir(BD)$

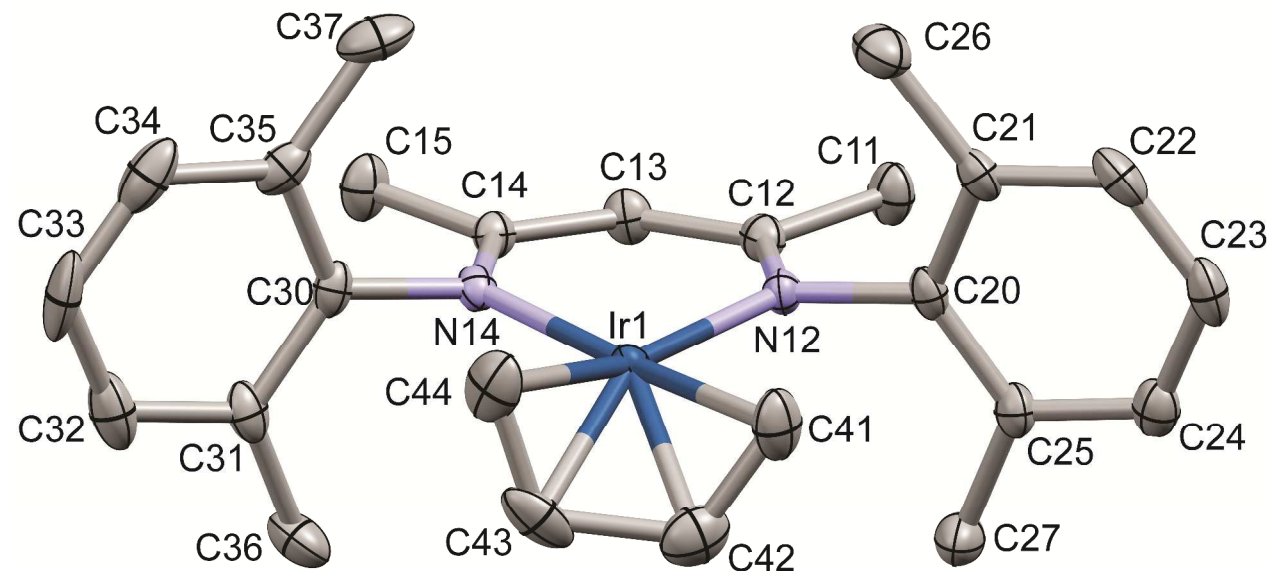


Figure S3. Crystal structure of $(^{Me}BDI)Ir(BD)$ (45% probability ellipsoids). Hydrogen atoms omitted for clarity.

Singlet and triplet geometries

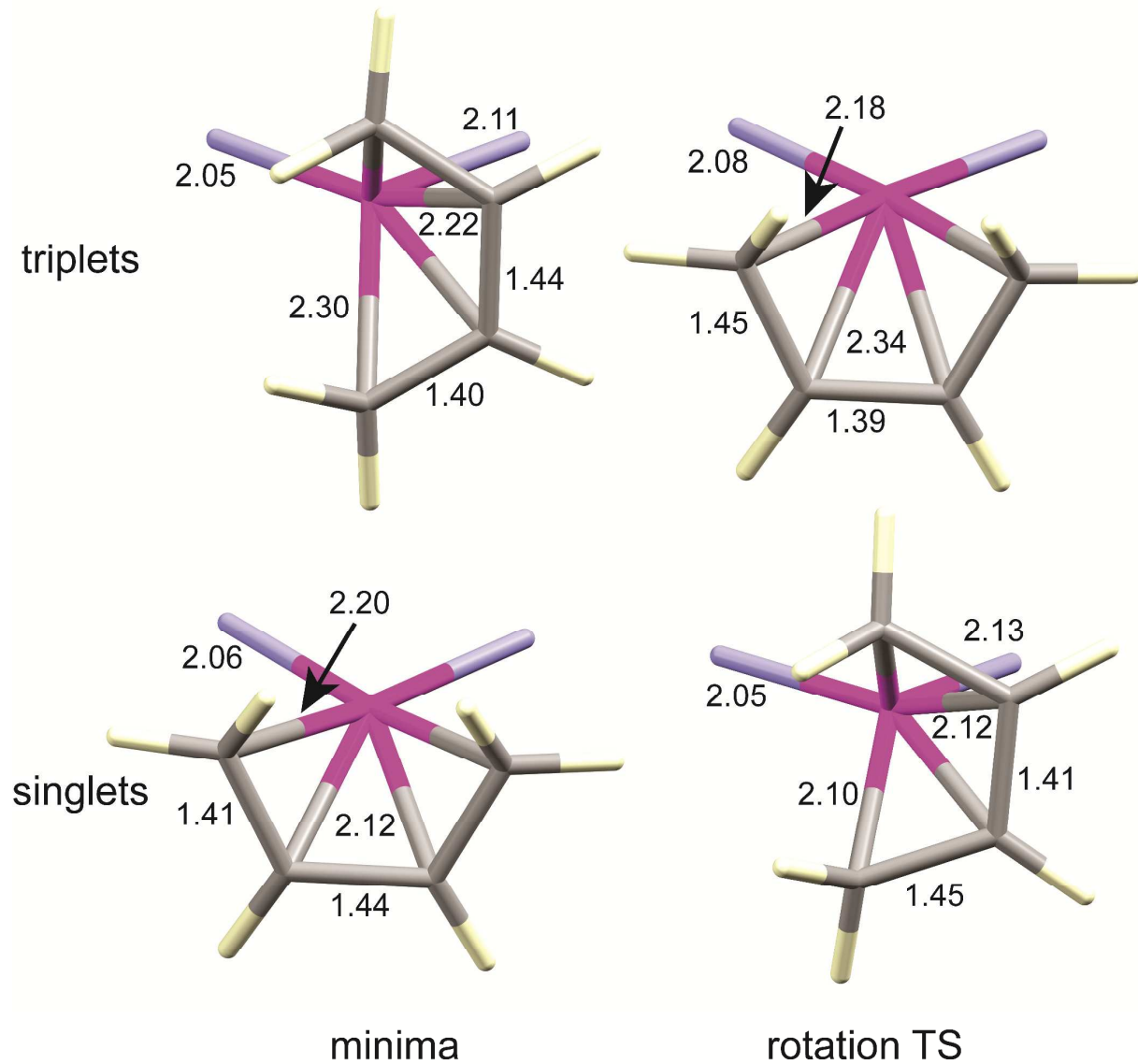
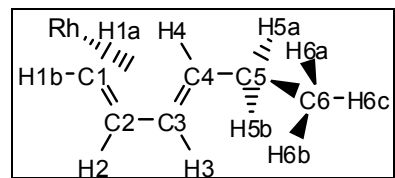


Figure S4. Comparison of optimized core geometries (at TPSSh/TZVP level) of $(^{Me}BDI)Rh(BD)$ in singlet and triplet states during diene rotation. Most of the ^{Me}BDI ligand omitted for clarity. Bond lengths in Å.

Comparison of calculated and observed NMR parameters

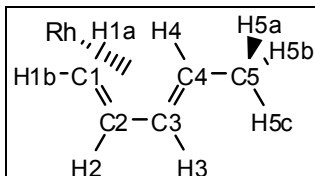
Chemical shifts (δ) in ppm relative to Me₄Si calculated at the same level. Coupling constants (J) in Hz.

Complex 1



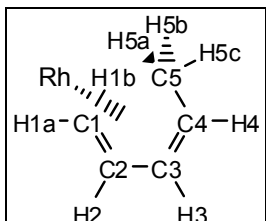
Shift	B3LYP	TPSSh	Observed	Coupling	B3LYP	TPSSh	Observed
C1	64.857	62.906	50.6	H1b-H1a	-1.1	0.4	~0
C2	79.329	76.312	76.5	H1b-H2	7.0	7.0	7.0
C3	99.225	95.209	87.5	H1a-H2	9.0	10.7	11.0
C4	79.144	75.273	70.5	H2-H3	4.7	4.5	4.5
C5	27.213	26.760	22.0	H3-H4	9.3	11.2	10.5
C6	20.023	19.891	15.3	H4-H5a	3.6	3.3	4
H1b	0.667	0.872	0.81	H4-H5b	10.3	11.9	11
H1a	1.220	1.429	0.55	H5a-H5b	-12.9	-13.1	13.0
H2	2.918	2.988	4.08	H5a-H6	7.1	7.6	7.5
H3	5.070	5.025	4.60	H5b-H6	6.9	7.4	7.5
H4	1.241	1.436	1.44				
H5a	-0.978	-0.887	-0.23				
H5b	0.153	0.224	-0.11				
H6	0.389	0.403	0.48				

Complex 2a



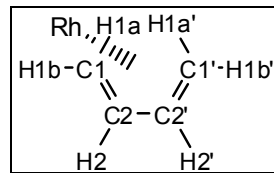
Shift	B3LYP	TPSSh	Observed	Coupling	B3LYP	TPSSh	Observed
C1	64.743	62.795	50.5	H1b-H1a	-1.2	0.3	~0
C2	79.055	76.045	76.2	H1b-H2	7.0	7.0	7.0
C3	99.467	95.457	88.3	H1a-H2	9.1	10.7	10.5
C4	72.153	69.132	63.8	H2-H3	4.7	4.5	4.5
C5	15.734	16.305	13.5	H3-H4	9.3	11.2	11.5
H1b	0.626	0.832	0.77	H4-H5	6.4	6.7	6.0
H1a	1.176	1.388	0.53				
H2	2.944	3.014	4.10				
H3	5.043	4.994	4.57				
H4	1.293	1.494	1.52				
H5	-0.216	-0.166	-0.43				

Complex 2b



Shift	B3LYP	TPSSh	Observed	Coupling	B3LYP	TPSSh	Observed
C1	67.200	64.741	52.8	H1b-H1a	-1.7	-0.3	~0
C2	89.243	85.379	83.1	H1b-H2	7.9	8.1	8.0
C3	89.138	85.739	77.7	H1a-H2	10.0	11.8	11.5
C4	80.867	77.557	n.o.	H2-H3	4.6	4.4	4.5
C5	19.594	20.095	14.3	H3-H4	8.4	8.6	7.5
H1b	0.131	0.327	0.82	H4-H5	7.0	7.4	7.0
H1a	2.028	2.175	1.54				
H2	4.107	4.117	4.62				
H3	4.457	4.492	3.88				
H4	0.553	0.744	1.63				
H5	0.780	0.816	0.42				

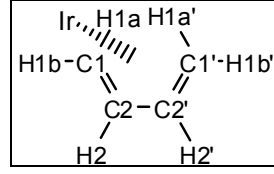
Complex 3 ^a



Shift	B3LYP	TPSSh	Observed	Coupling	B3LYP	TPSSh	Observed
C1	62.263	59.991	50.7	H1b-H1a	-1.6	-0.2	~0
C2	87.852	85.379	81.3	H1b-H2	7.1	7.2	6.5
H1b	0.056	0.245	0.68	H1a-H2	9.4	11.2	10.0
H1a	1.253	1.419	0.85	H2-H2'	4.3	4.1	
H2	4.328	4.326	4.36				

^a Symmetry-related values averaged.

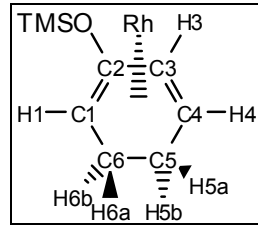
Complex 4 ^a



Shift	B3LYP	TPSSh	Observed	Coupling	B3LYP	TPSSh	Observed
C1	52.759	51.231	36.8	H1b-H1a	-2.2	-0.8	~0
C2	77.825	74.956	69.5	H1b-H2	6.7	6.8	~7
H1b	0.158	0.158	0.89	H1a-H2	8.3	9.8	~9
H1a	-0.030	1.020	-0.13	H2-H2'	3.7	3.4	
H2	3.907	3.950	4.19				

^a Symmetry-related values averaged.

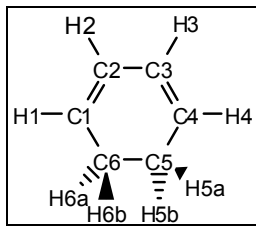
Complex 5



Shift	B3LYP	TPSSh	Observed	Coupling	B3LYP	TPSSh	Observed
C1	67.315	64.968	57.3	H1-H6b	5.0	5.0	4
C2	139.155	134.623	127.6	H1-H6a	2.1	1.9	2
C3	78.951	75.728	72.7	H3-H4	6.6	6.7	6.5
C4	82.102	79.177	68.4	H4-H5a	3.0	2.8	2.5
C5	30.279	30.058	24.5	H4-H5b	4.3	4.1	4

C6	24.183	24.376	21.2	H5a-H5b	-16.2	-16.5	25.5
H1	0.545	0.755	1.23	H5a-H6b	2.1	2.2	4
H3	3.058	3.146	3.46	H5a-H6a	9.2	9.4	9
H4	1.590	1.786	1.76	H5b-H6b	11.6	12.3	11.5
H5a	1.463	1.492	0.34	H5b-H6a	5.1	5.6	5
H5b	1.856	1.864	1.31	H6b-H6a	-13.9	-13.9	14
H6b	1.148	1.194	1.01				
H6a	1.068	1.099	0.52				

(EtBDI)Rh(1,3-CHD)^d

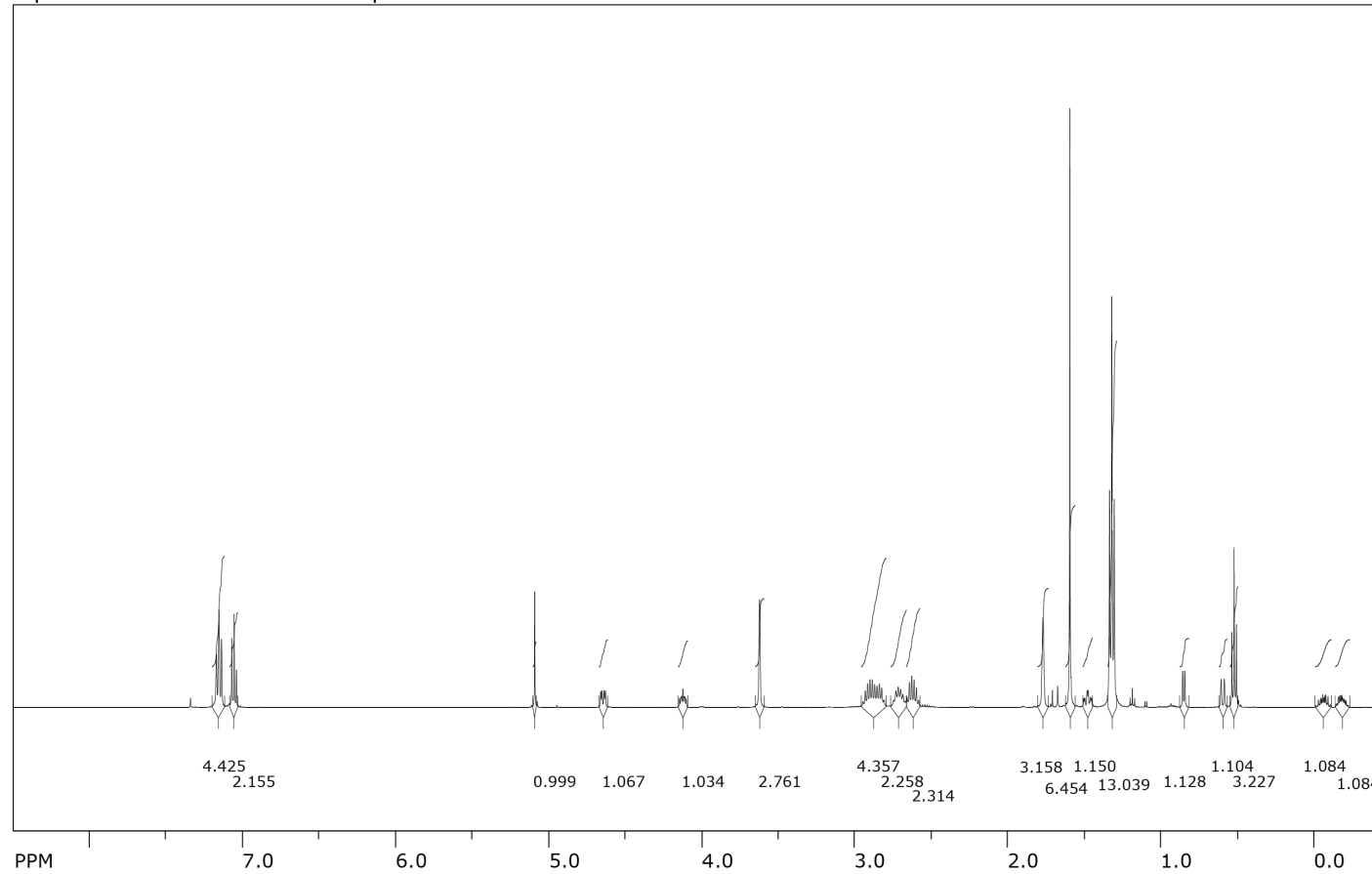


Shift	B3LYP	TPSSh	Observed ^a	Coupling	B3LYP	TPSSh	Observed ^c
C1	83.414	80.131	72.4	H1-H2	6.8	6.9	
C2	85.121	81.740	79.5	H1-H6a	4.7	4.6	
C5	26.977	26.887	24.5	H1-H6b	2.7	2.4	
H1	0.917	1.122	0.54 ^a	H2-H3	4.0	3.8	
H2	4.091	4.135	4.26	H5b-H6a	11.0	11.5	
H5a	1.298	1.317	1.37 ^b	H5b-H6b	3.8	4.1	
H5b	1.597	1.607	1.64 ^b	H6a-H6b	-15.6	-15.8	

^a Observed data for (^{Me}BDI)Rh(1,3-CHD) from: Budzelaar, P. H. M.; Moonen, N. N. P.; de Gelder, R.; Smits, J. M. M.; Gall, A. W., *Eur. J. Inorg. Chem.* **2000**, 753-769; Calculated data for (^{Et}BDI)Rh(1,3-CHD). ^b Assignment switched from original publication. ^c Couplings were not reported. ^d The CHD ring is slightly twisted and therefore has no symmetry, but inversion is fast. All listed values are averages between the two twisted conformations of the CHD ring.

NMR spectra for (^{Et}BDI)Rh(*trans*-1,3-HD)

SpinWorks 4: 298 K reference spectrum in THF-d₈



file: ..._data\rss-1-14_Lt EtBDIRhHxD\1\fid expt: <zg30>
transmitter freq.: 500.133089 MHz
time domain size: 65536 points
width: 10000.00 Hz = 19.9947 ppm = 0.152588 Hz/pt
number of scans: 16

freq. of 0 ppm: 500.130000 MHz
processed size: 65536 complex points
LB: 0.300 GF: 0.0000

Figure S5. ¹H NMR spectrum of (^{Et}BDI)Rh(*trans*-1,3-HD) (THF-*d*₈, 298K), overview.

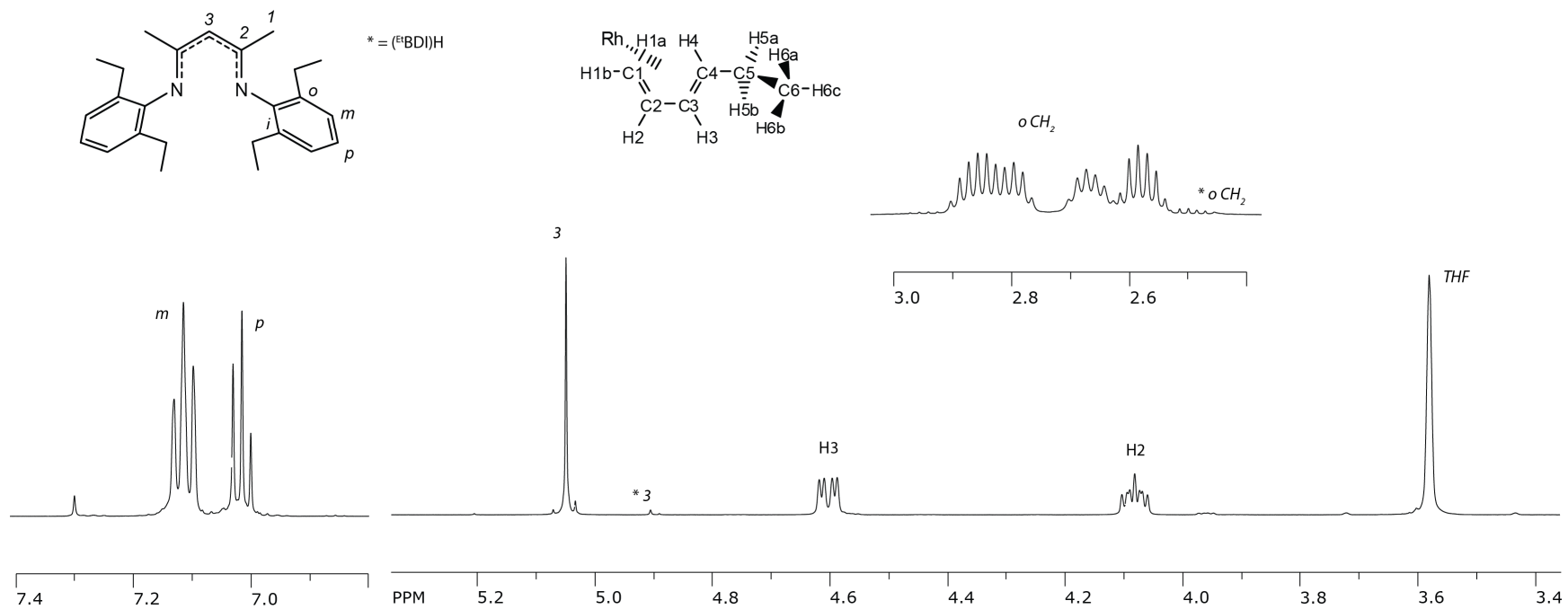


Figure S6. ^1H NMR spectrum of $(^{\text{Et}}\text{BDI})\text{Rh}(\text{trans-1,3-HD})$ (THF-*d*₈, 298K), assignments (part 1).

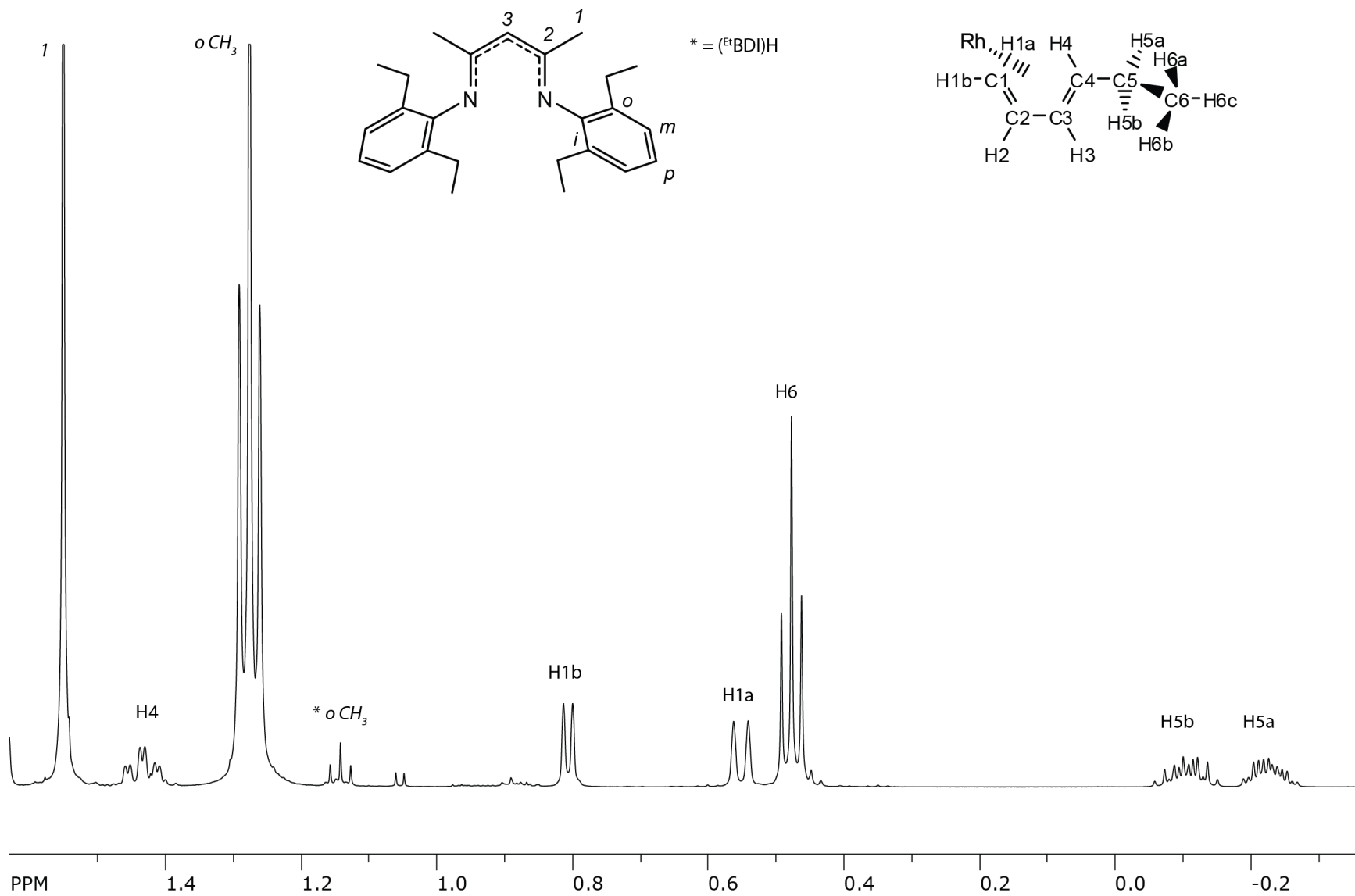
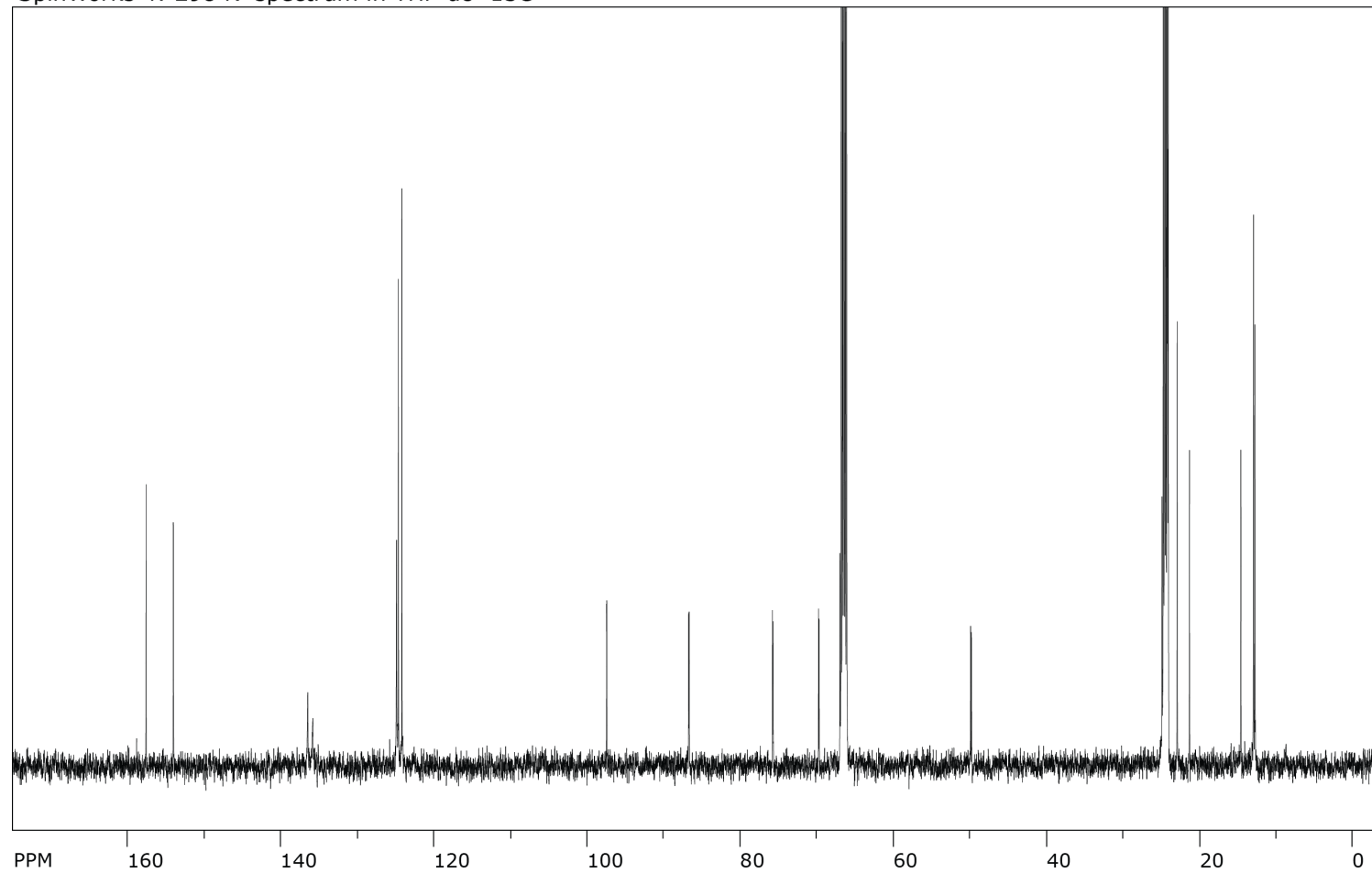


Figure S7. ^1H NMR spectrum of $(^{\text{Et}}\text{BDI})\text{Rh}(\text{trans-1,3-HD})$ (THF- d_8 , 298K), assignments (part 2).

SpinWorks 4: 298 K spectrum in THF-d₈ 13C



file: ...data\rss-1-14_It EtBDIRhHxD\10\fid expt: <zgpg30>
transmitter freq.: 125.770364 MHz
time domain size: 65536 points
width: 29761.91 Hz = 236.6369 ppm = 0.454131 Hz/pt
number of scans: 283

freq. of 0 ppm: 125.757789 MHz
processed size: 32768 complex points
LB: 2.000 GF: 0.0000

Figure S8. ¹³C NMR spectrum of (^{Et}BDI)Rh(*trans*-1,3-HD) (THF-*d*₈, 298K), overview.

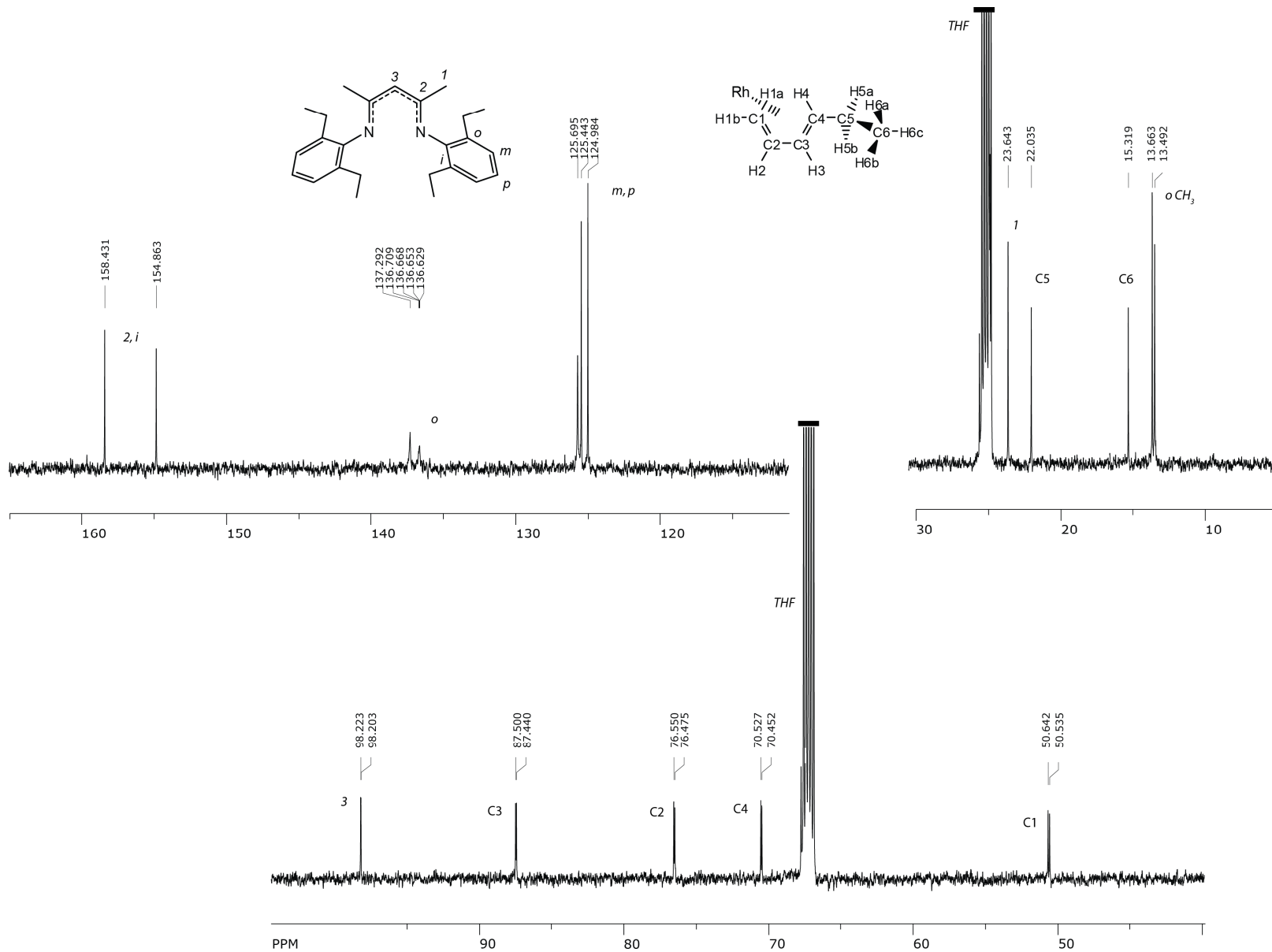


Figure S9. ^{13}C NMR spectrum of $(^{\text{Et}}\text{BDI})\text{Rh}(\text{trans-1,3-HD})$ ($\text{THF}-d_8$, 298K), assignments.

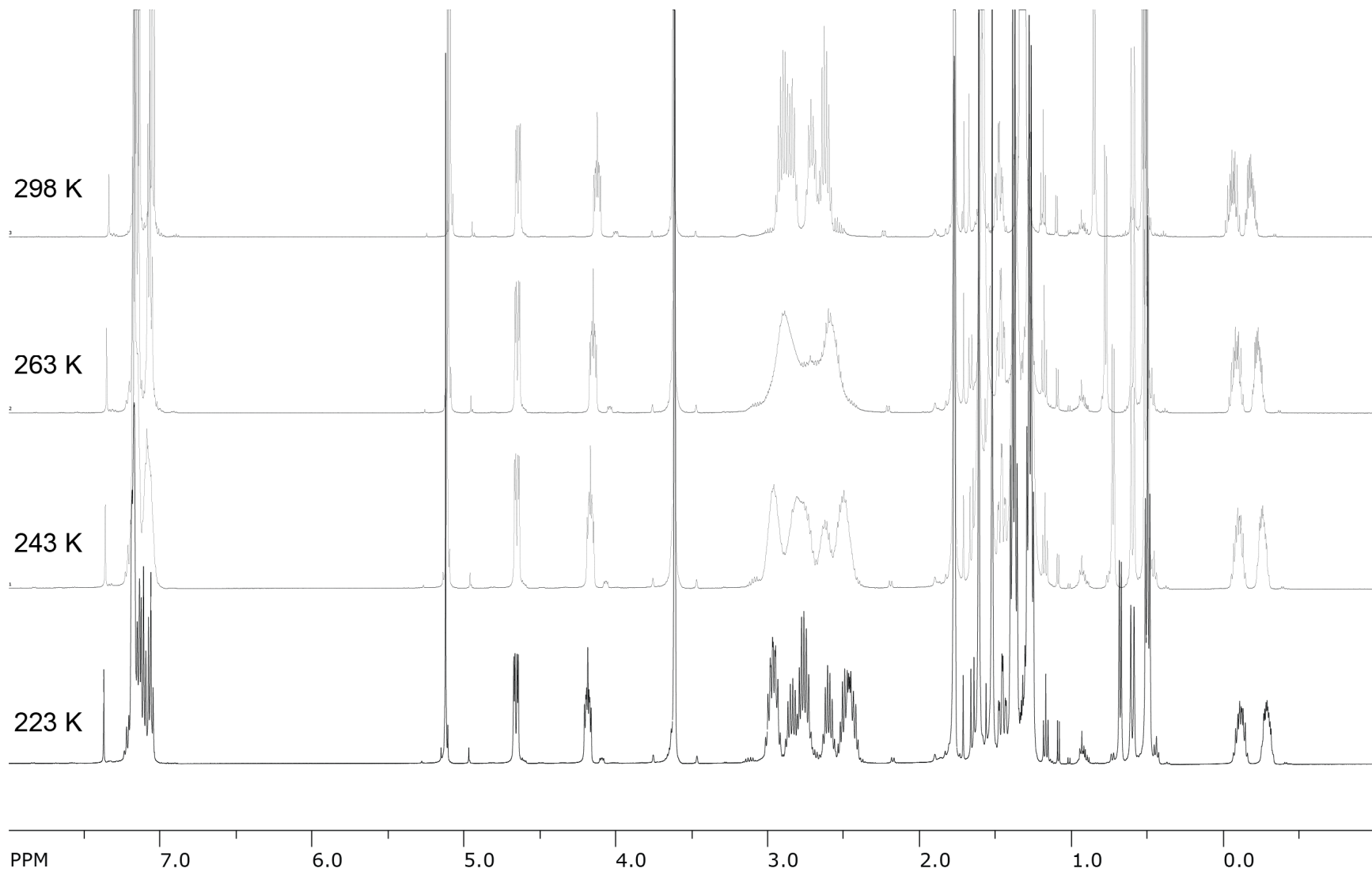
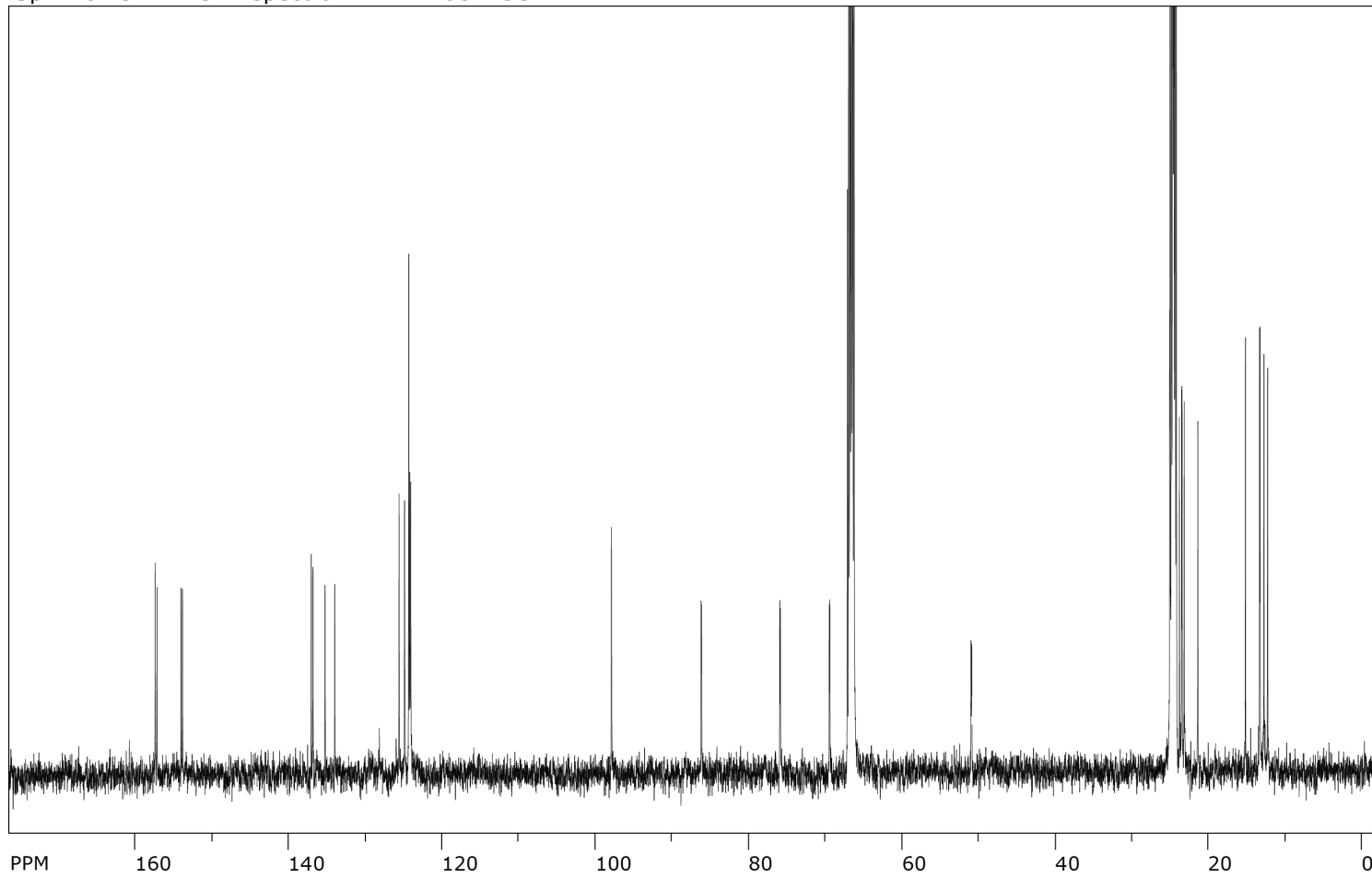


Figure S10. Selected ^1H VT-NMR spectra for $(\text{EtBDI})\text{Rh}(\text{trans-1,3-HD})$ ($\text{THF}-d_8$).

SpinWorks 4: 223 K spectrum in THF-d₈ 13C



file: ...-1-14_1t EtBDIRhHxD\223 carbon\fid expt: <zgpg30>
transmitter freq.: 125.770364 MHz
time domain size: 65536 points
width: 29761.91 Hz = 236.6369 ppm = 0.454131 Hz/pt
number of scans: 176

freq. of 0 ppm: 125.757789 MHz
processed size: 32768 complex points
LB: 2.000 GF: 0.0000

Figure S11. ¹³C NMR spectrum of (^{Et}BDI)Rh(*trans*-1,3-HD) (THF-*d*₈, 223K), overview.

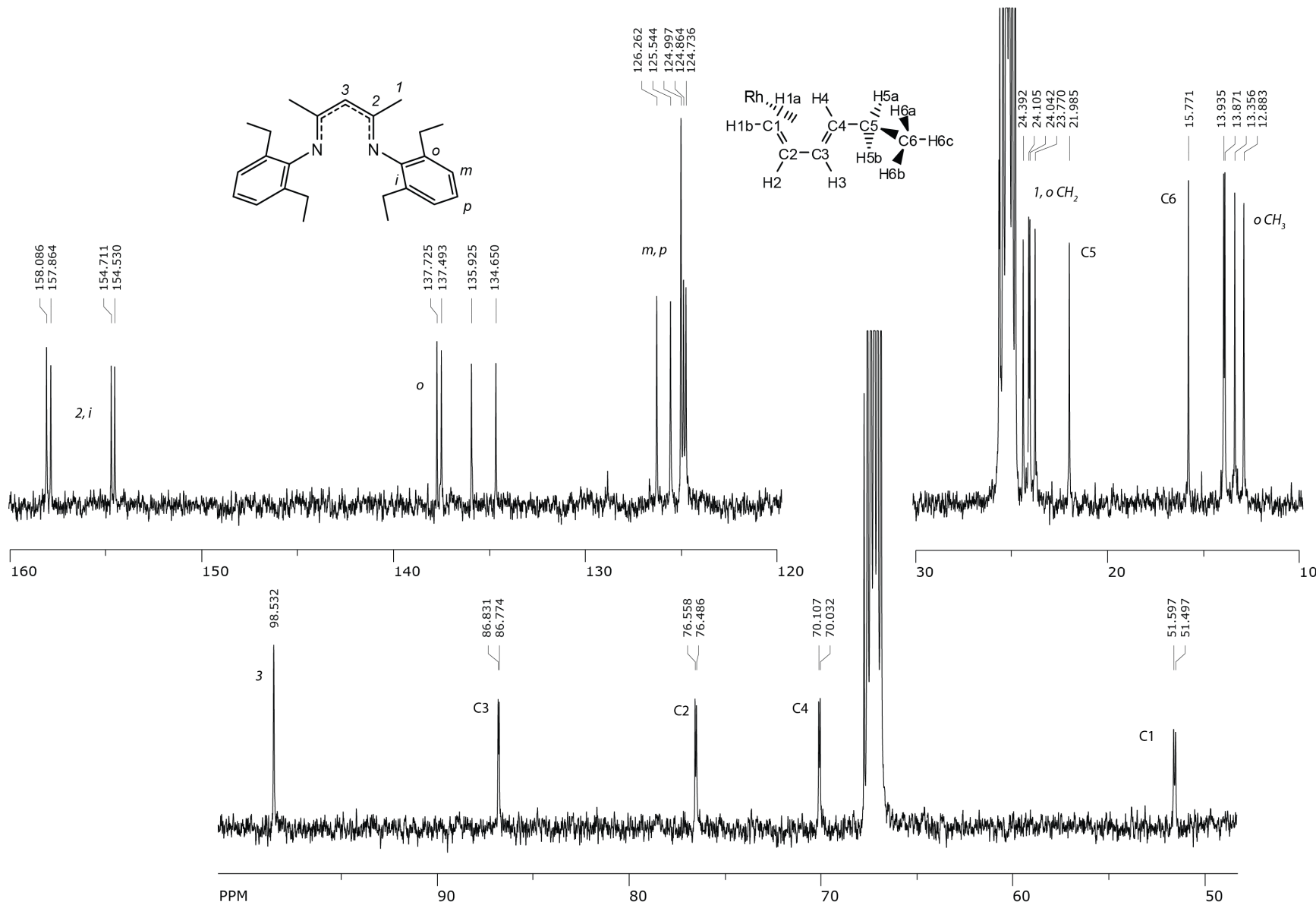
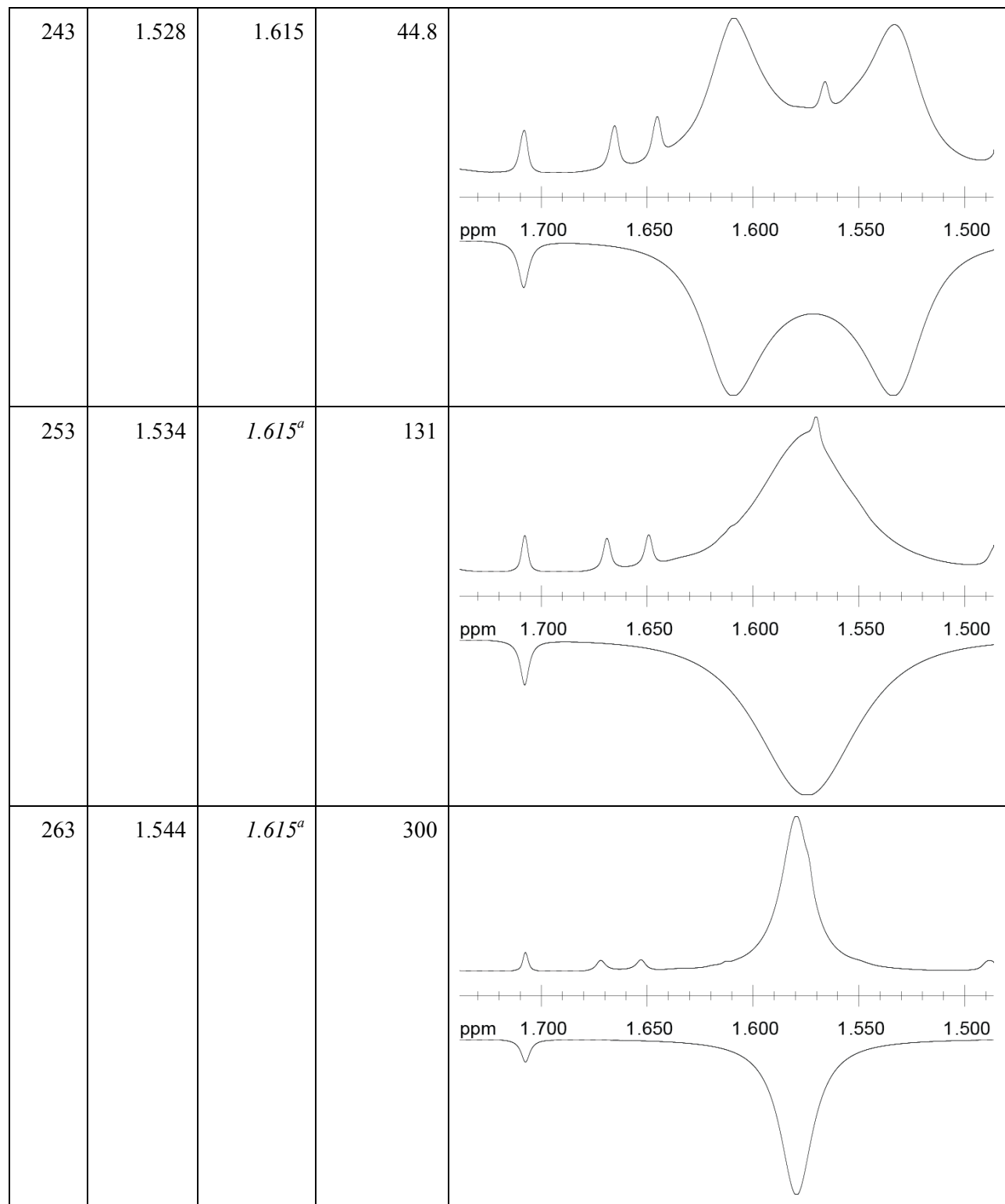


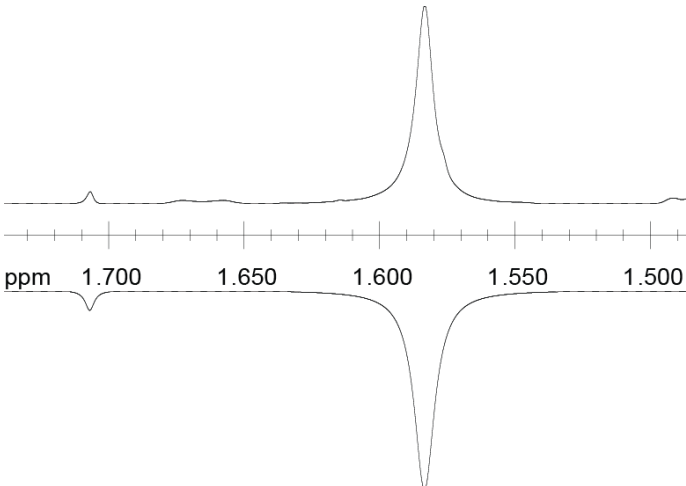
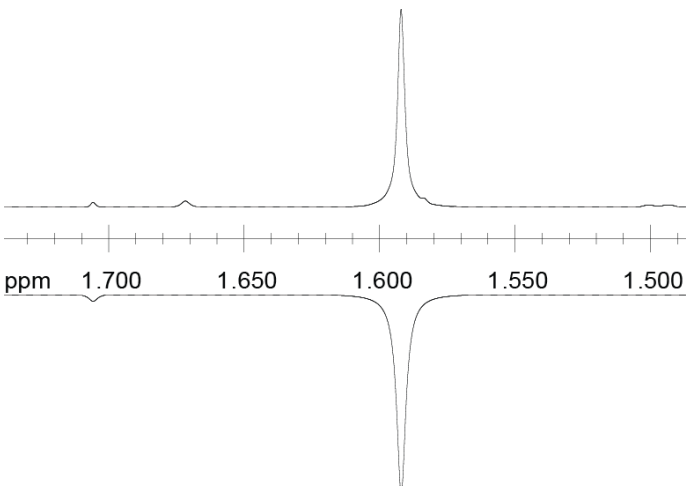
Figure S12. ^{13}C NMR spectrum of $(\text{Et}^{\text{t}}\text{BDI})\text{Rh}(\text{trans-1,3-HD})$ (THF- d_8 , 223K), assignments.

Simulation of VT-NMR spectra, (^{Et}BDI)Rh(*trans*-1,3-HD), imine methyl region.

Table S4. Chemical shifts of imine methyl groups, fitted rate constants, and fitted spectrum traces for VT-NMR spectra of (^{Et}BDI)Rh(*trans*-1,3-HD).

<i>T</i> (K)	δ_1 (ppm)	δ_2 (ppm)	<i>k</i> (mol L ⁻¹)	Fitted spectrum ^b
223	1.519	1.607	~0	<p style="text-align: center;">ppm 1.700 1.650 1.600 1.550 1.500</p>
233	1.523	1.610	11.7	<p style="text-align: center;">ppm 1.700 1.650 1.600 1.550 1.500</p>



273	1.552	<i>1.615^a</i>		626	
298	1.569	<i>1.615^a</i>	~inf		

^a δ_2 fixed in these lineshape fits. ^b Peak near 1.71 ppm is free (^{Et}BDI)H, fitted concentration about 4 mol%; peaks near 1.65 and 1.67 ppm at low temperature are traces of a second isomer, likely (^{Et}BDI)Rh(*cis*-1,3-HD), not included in the lineshape fit.

Eyring plot

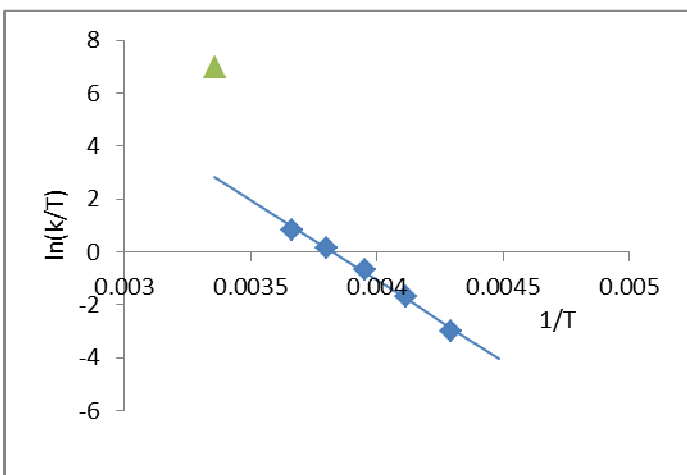


Figure S13. Eyring plot ($\ln k/T$ vs $1/T$) for (^{Et}BDI)Rh(trans-1,3-HD) over the range 233-273 K.

Fit results:

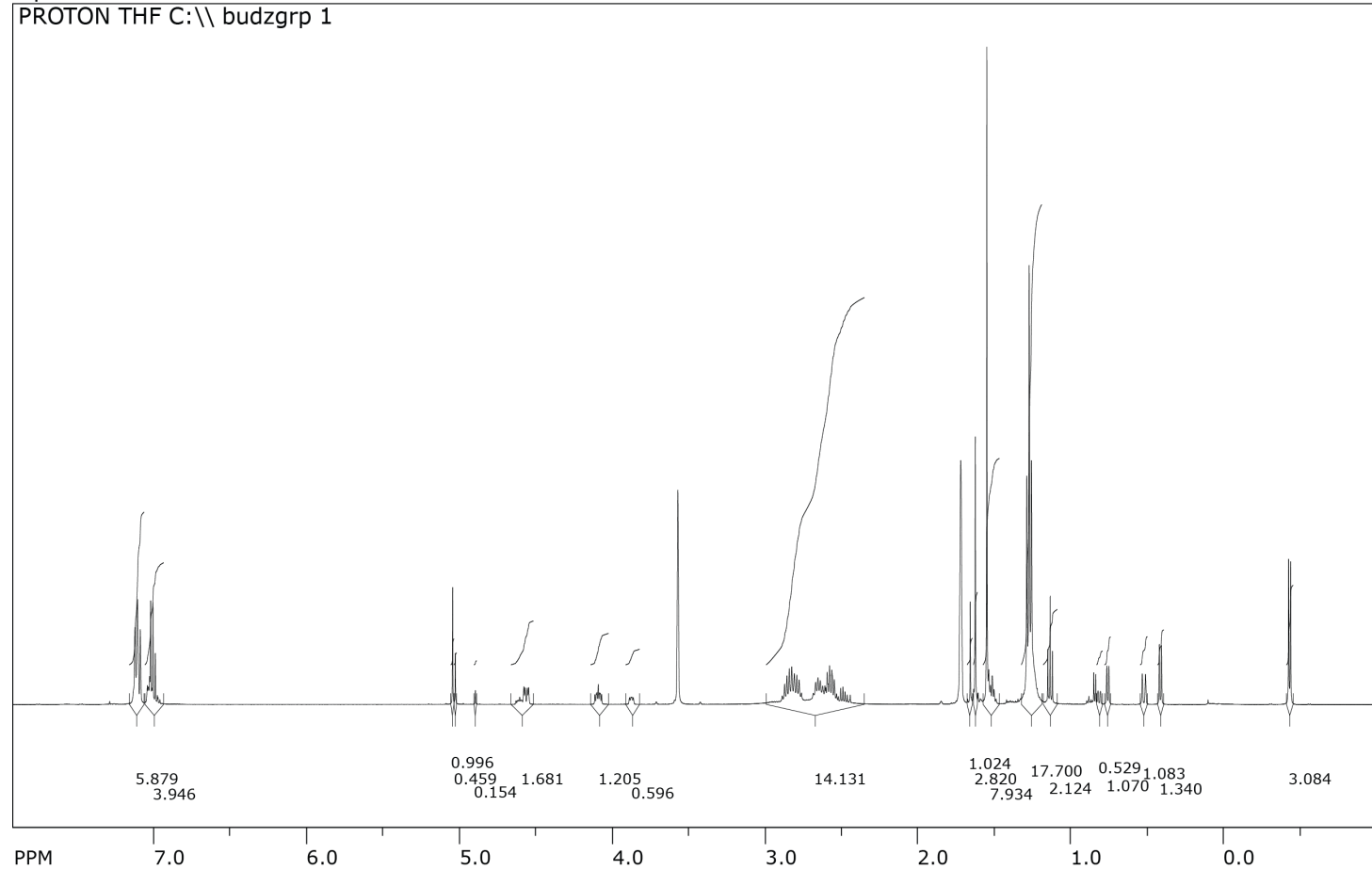
$$\Delta H^\ddagger = 50.3 \pm 2.4 \text{ kJ mol}^{-1} \quad 12.0 \pm 0.6 \text{ kcal mol}^{-1}$$

$$\Delta S^\ddagger = -5.4 \pm 9.7 \text{ J mol}^{-1} \text{ K}^{-1} \quad -1.3 \pm 2.3 \text{ cal mol}^{-1} \text{ K}^{-1}$$

NMR spectra for (^{Et}BDI)Rh(*trans/cis*-1,3-PD)

SpinWorks 4: RSS-1-91 PnD

PROTON THF C:\\\\ budzgrp 1



file: ...nal_data\\RSS-1-91 EtBDIRhPnD\\1\\fid expt: <zg30>
transmitter freq.: 500.133089 MHz
time domain size: 65536 points
width: 10000.00 Hz = 19.9947 ppm = 0.152588 Hz/pt
number of scans: 16

freq. of 0 ppm: 500.129096 MHz
processed size: 65536 complex points
LB: 0.300 GF: 0.0000

Figure S14. ¹H NMR spectrum of (^{Et}BDI)Rh(*trans/cis*-1,3-PD) (THF-*d*₈, 298K), overview.

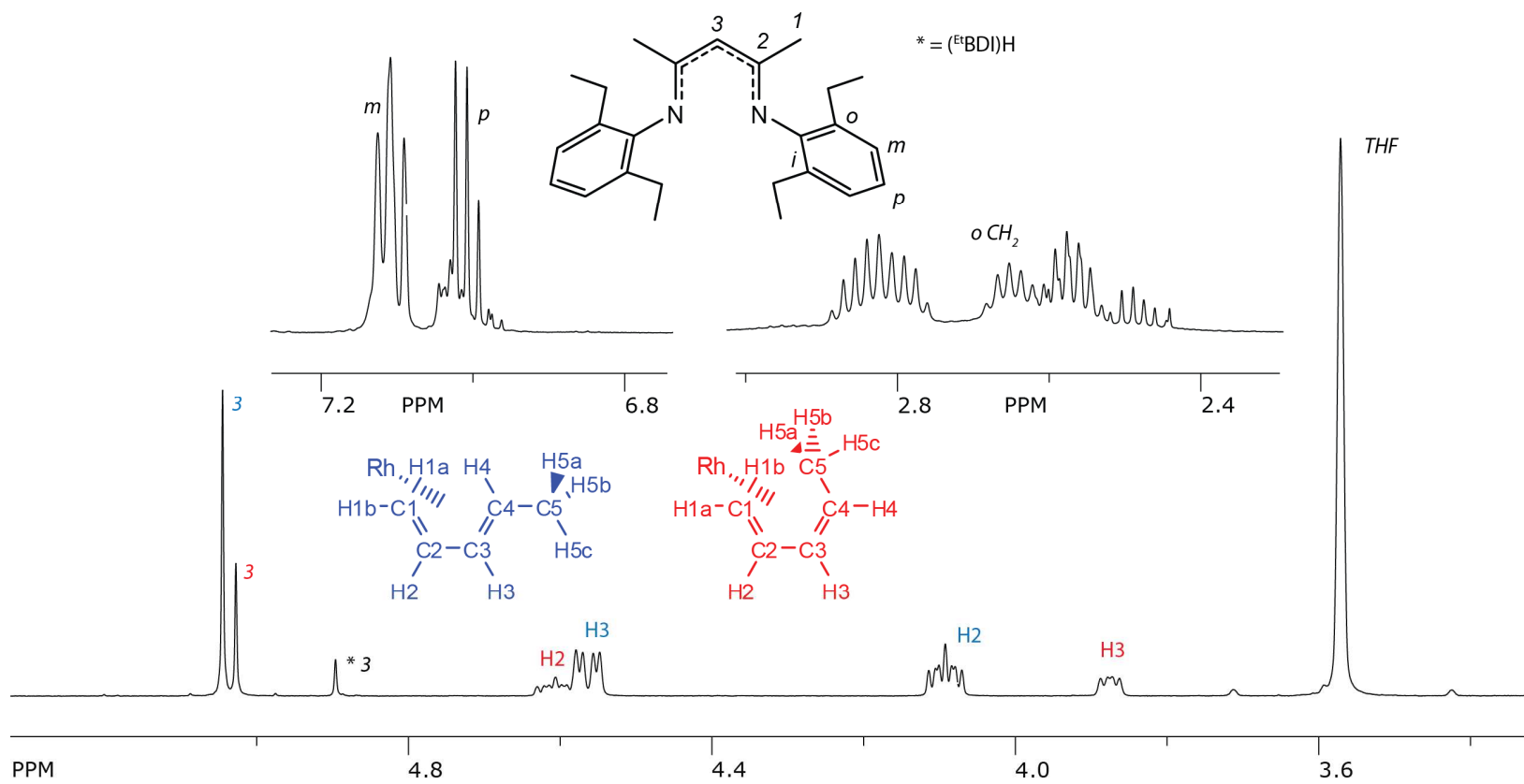


Figure S15. ^1H NMR spectrum of $(^{\text{Et}}\text{BDI})\text{Rh}(\text{trans/cis-1,3-PD})$ ($\text{THF}-d_8$, 298K), assignments (part 1).

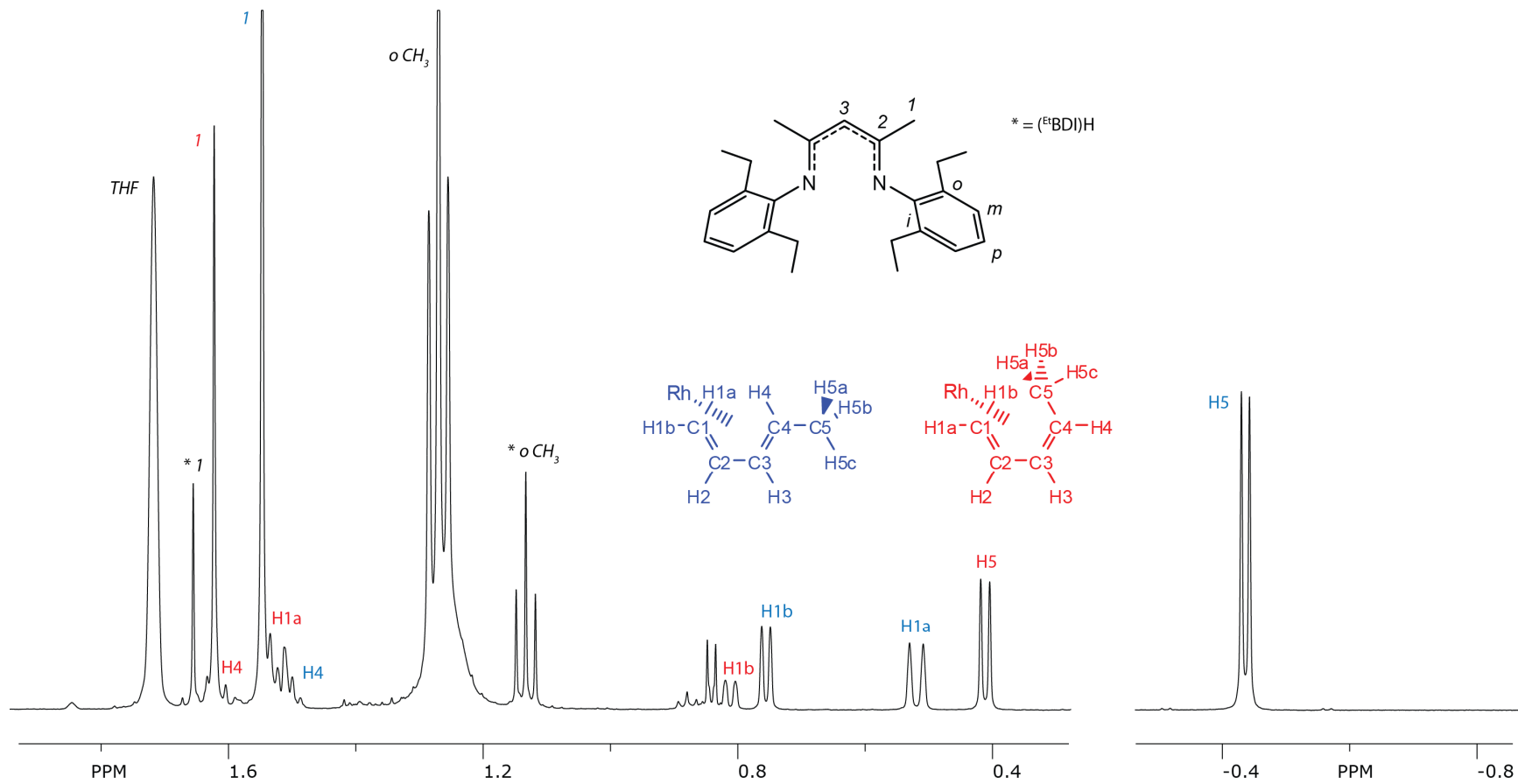
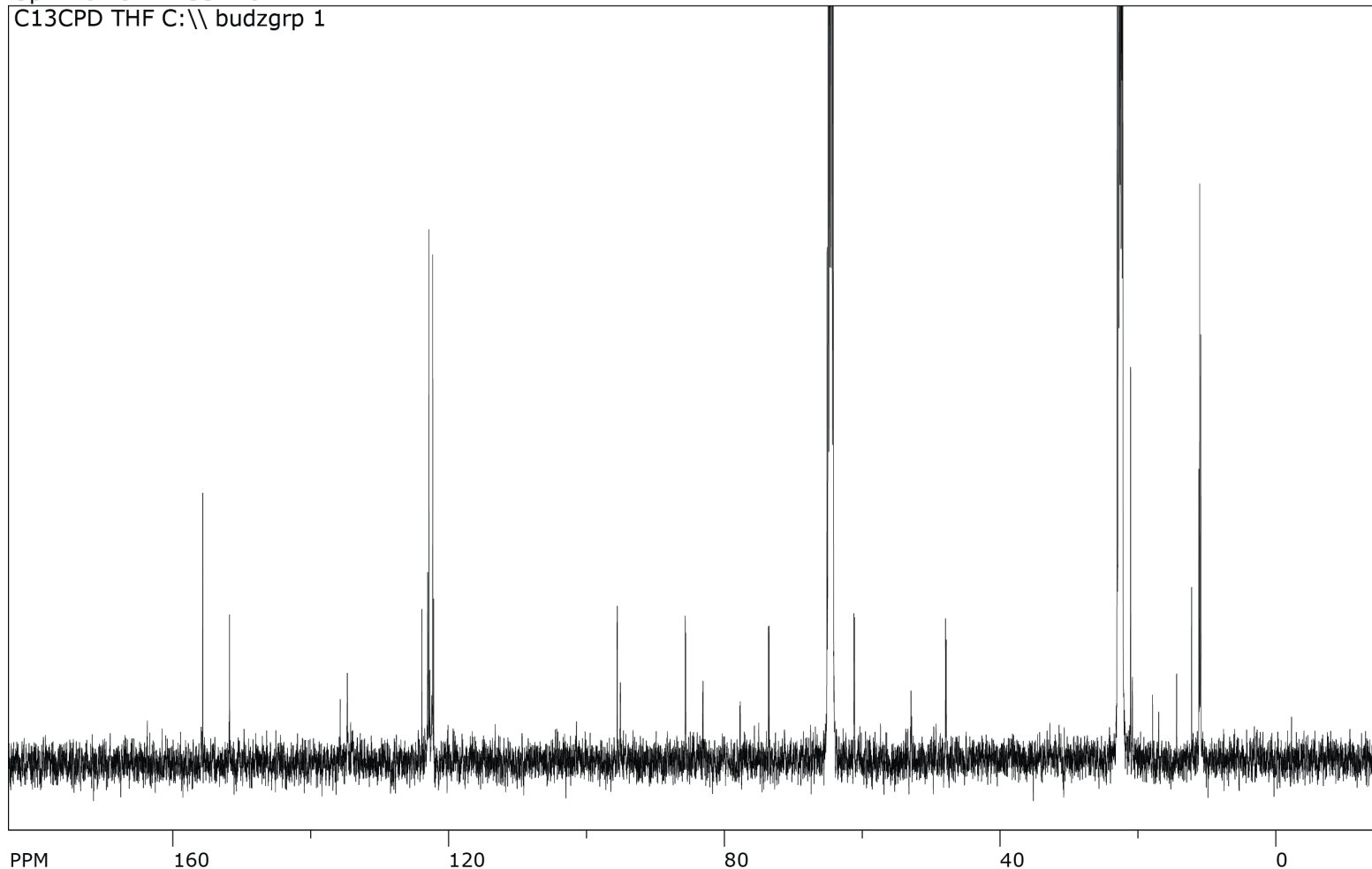


Figure S16. ^1H NMR spectrum of $(^{\text{Et}}\text{BDI})\text{Rh}(\text{trans/cis-1,3-PD})$ ($\text{THF}-d_8$, 298K), assignments (part 2).

SpinWorks 4: RSS-1-91 PnD
C13CPD THF C:\\ budzgrp 1



file: ...nal_data\\RSS-1-91 EtBDIRhPnD\\2\\fid expt: <zgpg30>
transmitter freq.: 125.770364 MHz
time domain size: 65536 points
width: 29761.91 Hz = 236.6369 ppm = 0.454131 Hz/pt
number of scans: 1024

freq. of 0 ppm: 125.757789 MHz
processed size: 32768 complex points
LB: 2.000 GF: 0.0000

Figure S17. ¹³C NMR spectrum of (^{Et}BDI)Rh(*trans/cis*-1,3-PD) (THF-*d*₈, 298K), overview.

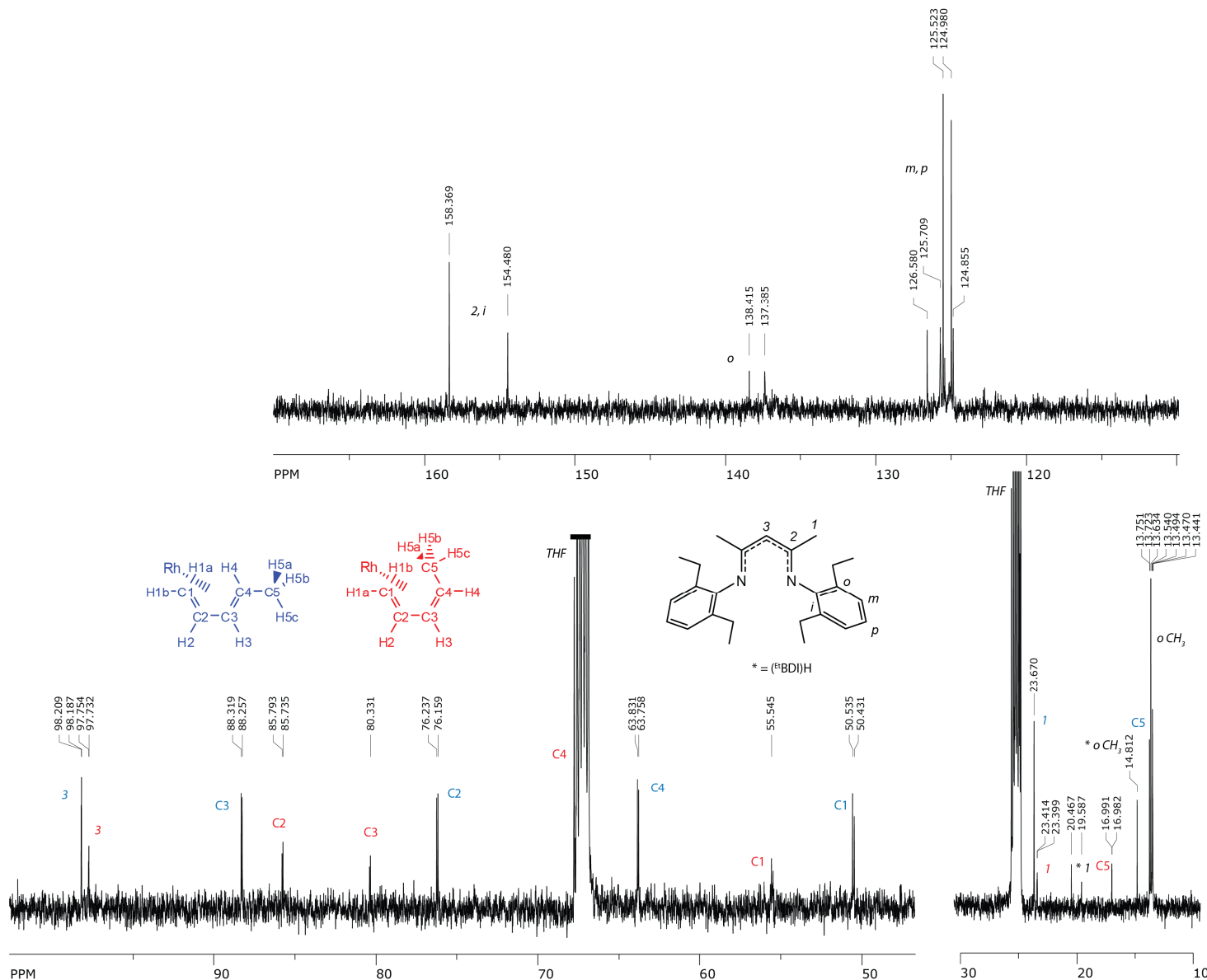


Figure S18. ^{13}C NMR spectrum of $(\text{Et}^{\text{t}}\text{BDI})\text{Rh}(\text{trans/cis-1,3-PD})$ ($\text{THF}-d_8$, 298K), assignments.

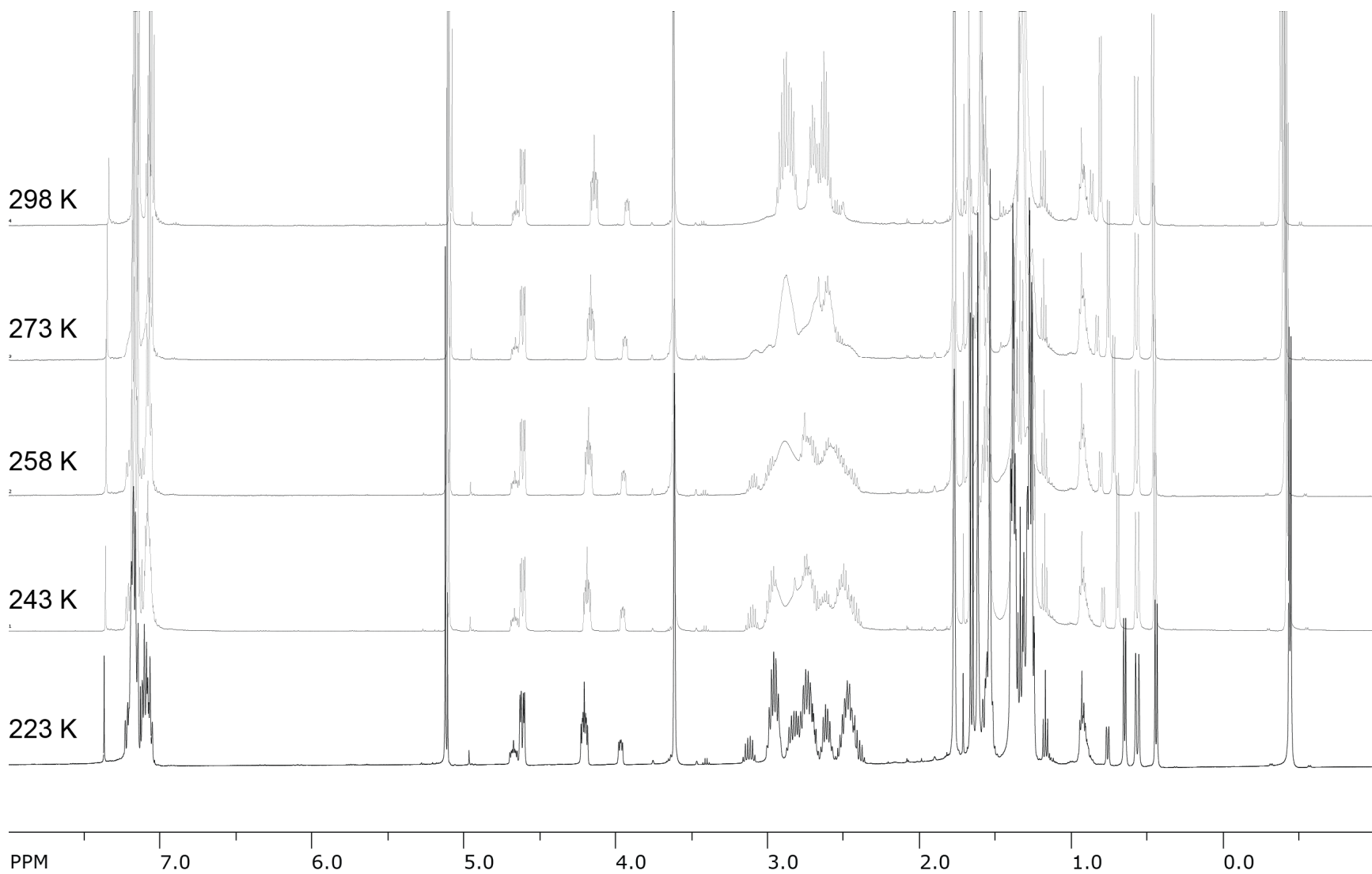
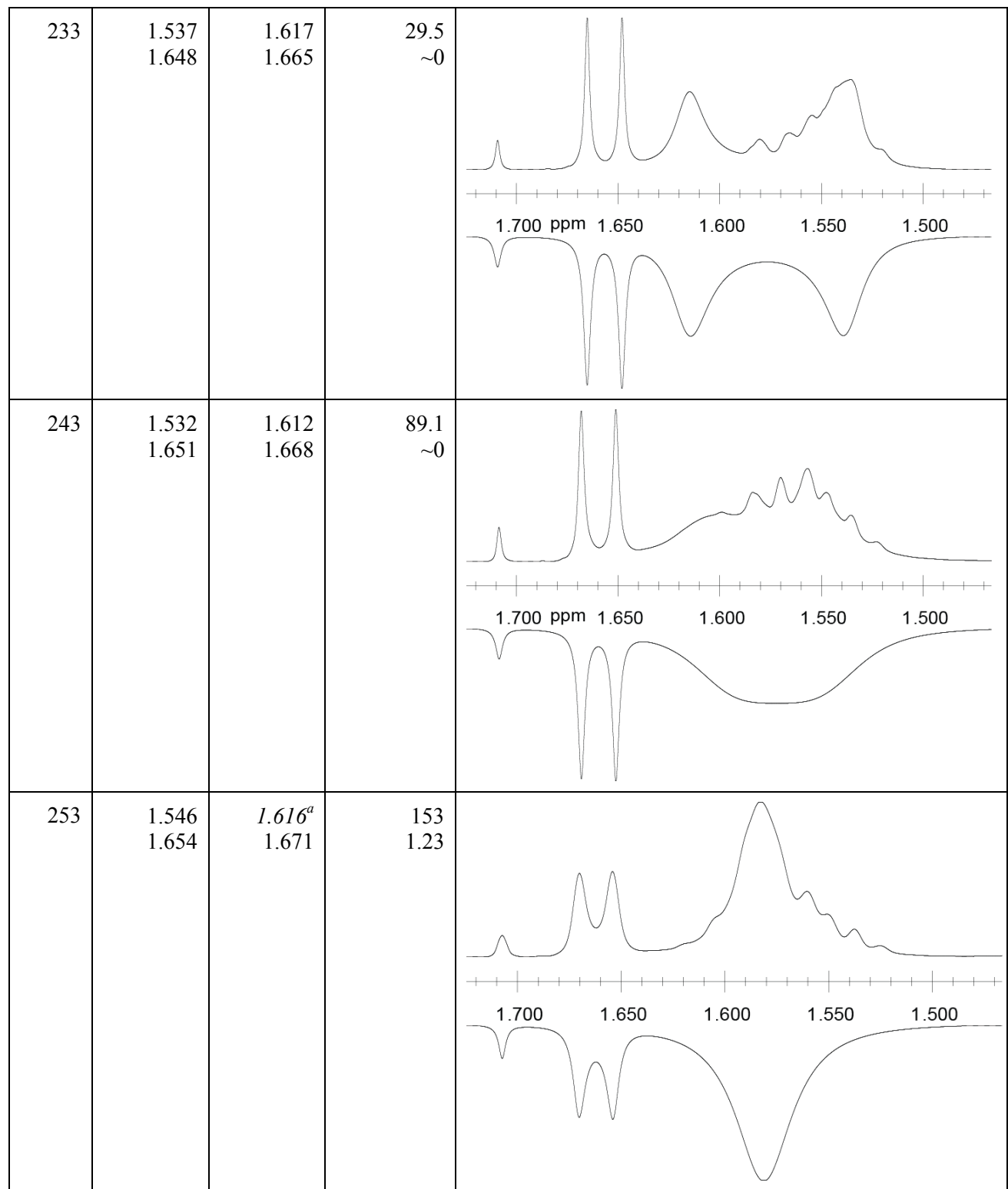


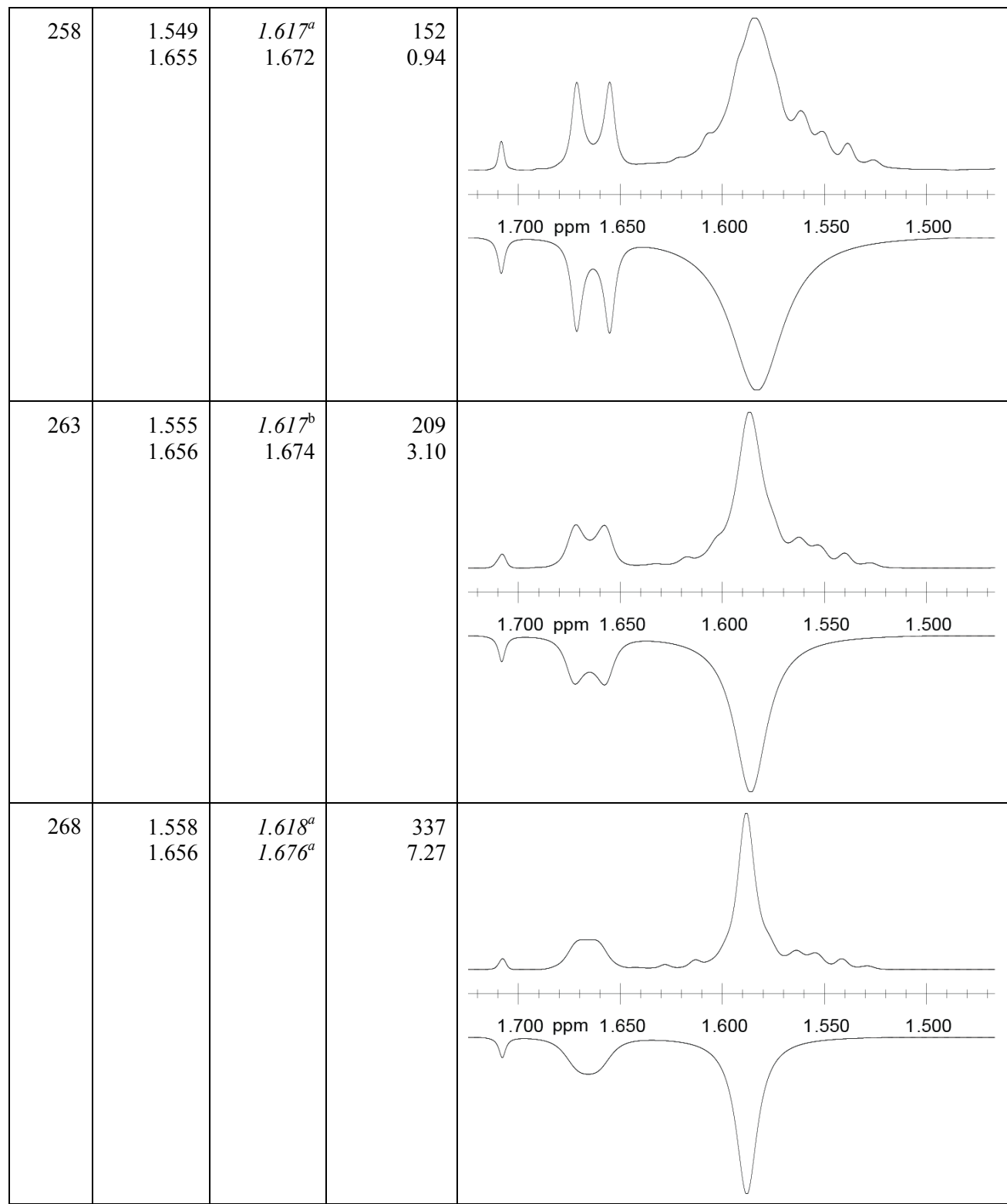
Figure S19. Selected ^1H VT-NMR spectra for $(^{\text{Et}}\text{BDI})\text{Rh}(\text{trans/cis-1,3-PD})$ ($\text{THF-}d_8$).

Simulation of VT-NMR spectra, (^{Et}BDI)Rh(*trans/cis*-1,3-PD), imine methyl region.

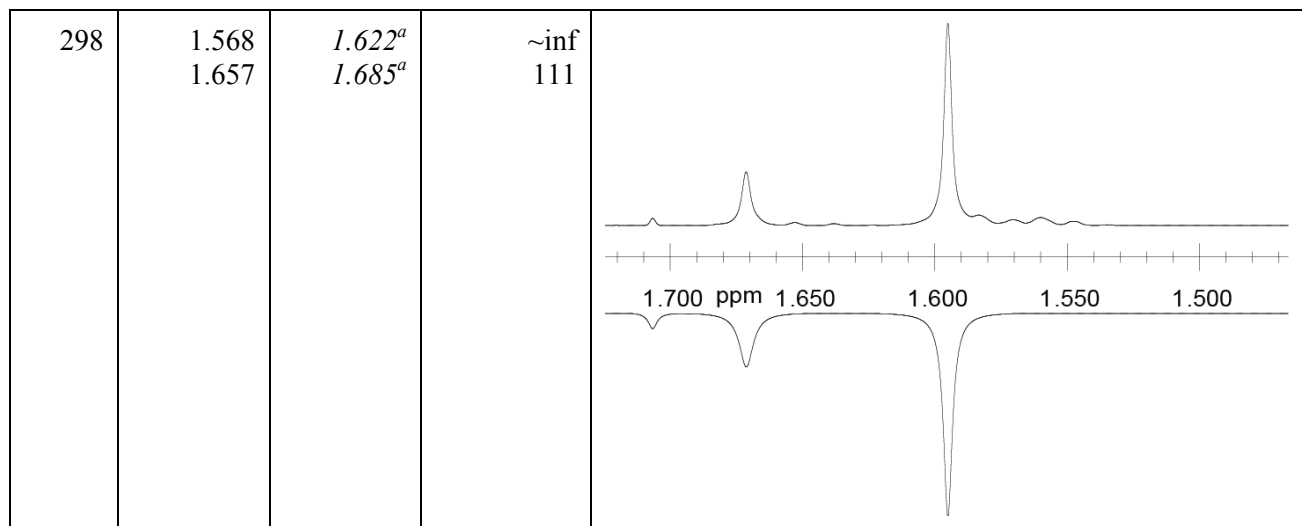
Table S5. Chemical shifts of imine methyl groups, fitted rate constants, and fitted spectrum traces for VT-NMR spectra of (^{Et}BDI)Rh(*trans/cis*-1,3-PD).

<i>T</i> (K)	δ_1 (ppm): <i>trans</i> <i>cis</i>	δ_2 (ppm): <i>trans</i> <i>cis</i>	<i>k</i> (mol L ⁻¹)	Fitted spectrum ^b
213	1.527 1.641	1.609 1.658	~0 ~0	
223	1.532 1.645	1.613 1.662	9.94 ~0	





273	1.561 1.657	<i>1.619^a</i> <i>1.677^a</i>	589 11.6	<p>Detailed description: This panel shows a 1H NMR spectrum for entry 273. The x-axis is labeled with chemical shifts in ppm: 1.700, 1.650, 1.600, 1.550, and 1.500. There are four distinct signals: a small peak at ~1.70 ppm, a broad peak at ~1.65 ppm, a sharp peak at ~1.60 ppm, and a very large, sharp peak at ~1.55 ppm.</p>
278	1.565 1.659	<i>1.619^a</i> <i>1.679^a</i>	1760 23.1	<p>Detailed description: This panel shows a 1H NMR spectrum for entry 278. The x-axis is labeled with chemical shifts in ppm: 1.700, 1.650, 1.600, 1.550, and 1.500. There are four distinct signals: a small peak at ~1.70 ppm, a broad peak at ~1.65 ppm, a sharp peak at ~1.60 ppm, and a very large, sharp peak at ~1.55 ppm.</p>
288	1.569 1.660	<i>1.621^a</i> <i>1.682^a</i>	~inf 49.6	<p>Detailed description: This panel shows a 1H NMR spectrum for entry 288. The x-axis is labeled with chemical shifts in ppm: 1.700, 1.650, 1.600, 1.550, and 1.500. There are four distinct signals: a small peak at ~1.70 ppm, a broad peak at ~1.65 ppm, a sharp peak at ~1.60 ppm, and a very large, sharp peak at ~1.55 ppm.</p>



^a δ_2 extrapolated from lower-temperature spectra for these lineshape fits. ^b Peak near 1.71 ppm is free (^{Et}BDI)H, fitted concentrations 70 mol% *trans*, 26 mol% *cis*, 4 mol% (^{Et}BDI)H; broader peaks in the range of 1.48-1.58 ppm are due to the diene ligand, not included in the lineshape fit.

Eyring plot for *trans* isomer

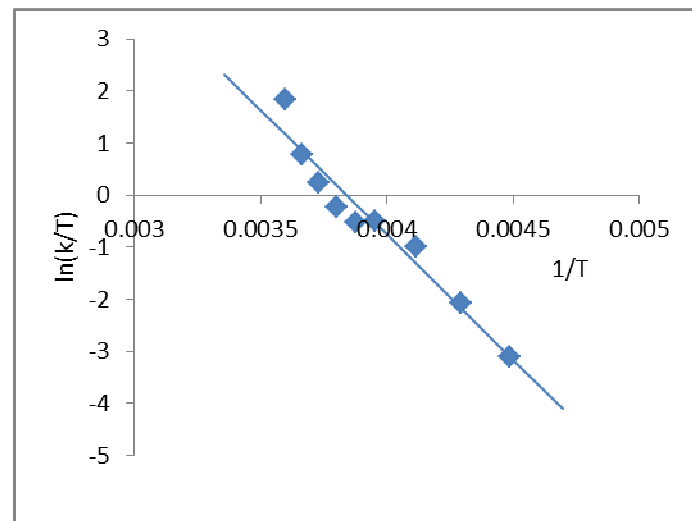


Figure S20. Eyring plot ($\ln k/T$ vs $1/T$) for (^{Et}BDI)Rh(*trans*-1,3-PD) over the range 223-278 K.

Fit results:

$$\Delta H^\ddagger = 39.8 \pm 3.7 \text{ kJ mol}^{-1} \quad 9.5 \pm 0.9 \text{ kcal mol}^{-1}$$

$$\Delta S^\ddagger = -44.9 \pm 14.5 \text{ J mol}^{-1} \text{ K}^{-1} \quad -10.7 \pm 3.5 \text{ cal mol}^{-1} \text{ K}^{-1}$$

Eyring plot for *cis* isomer

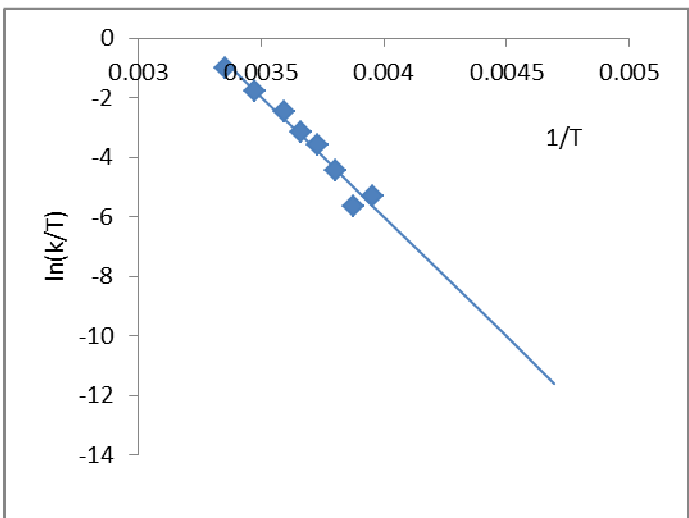


Figure S21. Eyring plot ($\ln k/T$ vs $1/T$) for $(^{Et}BDI)Rh(cis\text{-}1,3\text{-PD})$ over the range 253-298 K.

Fit results:

$$\Delta H^\ddagger = \quad 67.1 \pm 5.2 \quad \text{kJ mol}^{-1} \quad 16.0 \pm 1.2 \quad \text{kcal mol}^{-1}$$

$$\Delta S^\ddagger = \quad 21.0 \pm 19.2 \quad \text{J mol}^{-1} \text{K}^{-1} \quad 5.0 \pm 4.6 \quad \text{cal mol}^{-1} \text{K}^{-1}$$

NMR spectra for (^{Me}BDI)Rh(BD)

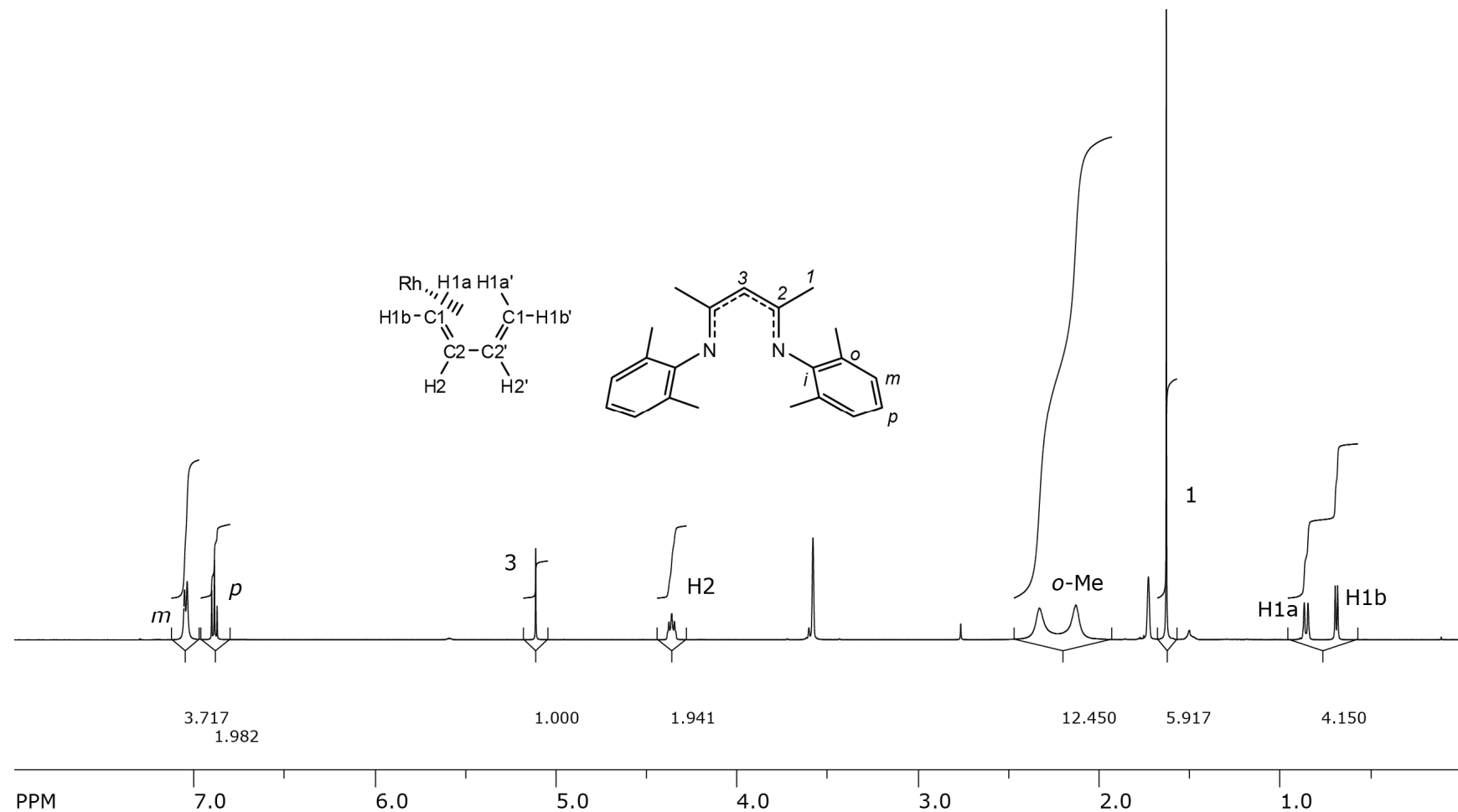


Figure S22. ¹H NMR spectrum of (^{Me}BDI)Rh(BD) (THF-*d*₈, 298K).

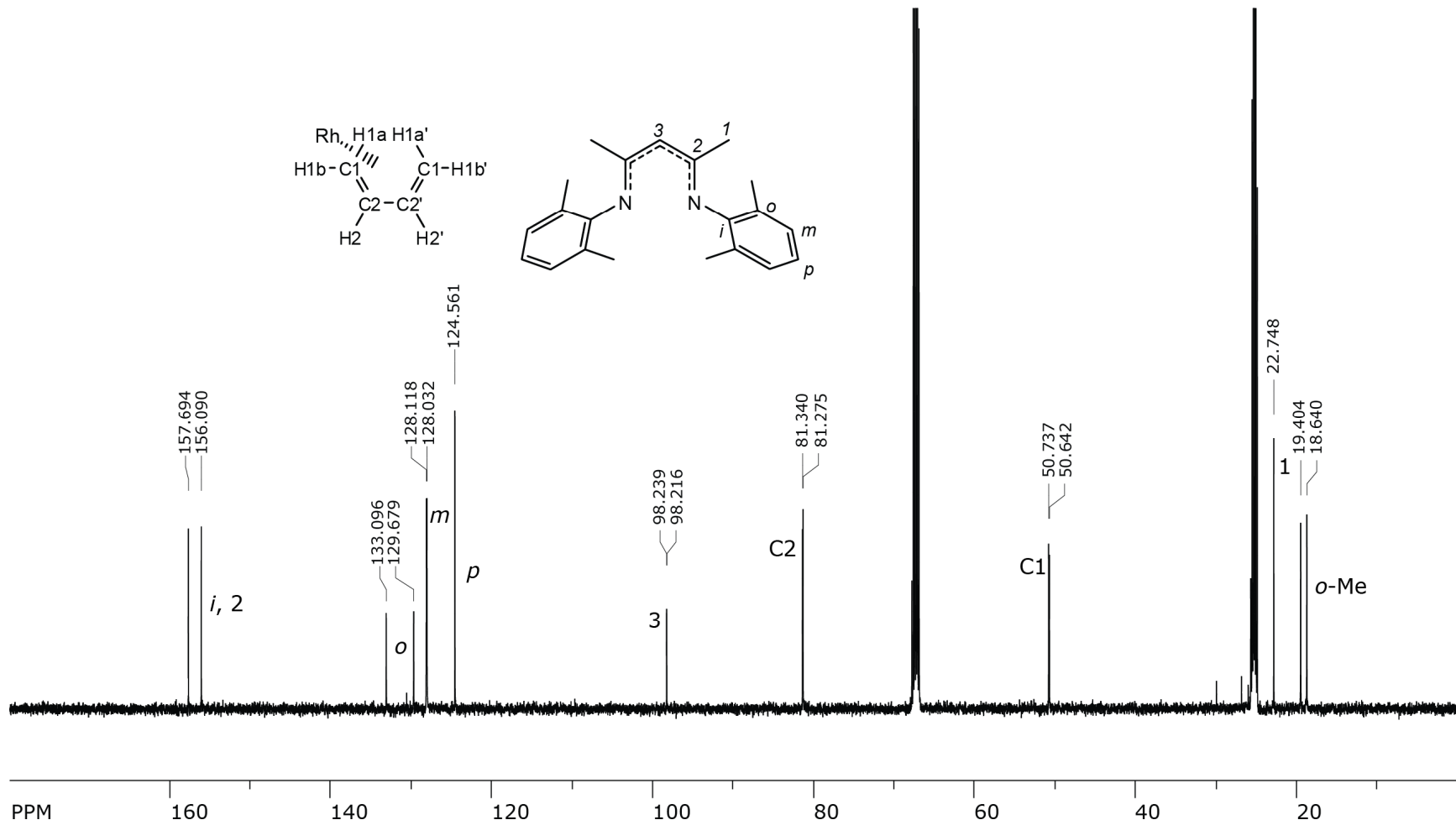


Figure S23. ^{13}C NMR spectrum of $(^{\text{Me}}\text{BDI})\text{Rh}(\text{BD})$ (THF- d_8 , 268K).

Simulation of VT-NMR spectra, (^{Me}BDI)Rh(BD), aryl methyl region.

Table S6. Fitted rate constants for VT-NMR spectra of (^{Me}BDI)Rh(BD).

T (K)	k (mol L ⁻¹)	1/T	ln(k/T)	pred ln(k/T)
273	~0	0.00366		-4.174
278	3.77	0.00360	-4.301	-3.628
283	10.7	0.00353	-3.275	-3.101
288	20.8	0.00347	-2.628	-2.592
293	37.8	0.00341	-2.048	-2.101
298	63.4	0.00336	-1.548	-1.627
303	106	0.00330	-1.050	-1.168
308	163	0.00325	-0.636	-0.723
313	244	0.00319	-0.249	-0.294
318	358	0.00314	0.118	0.123
323	534	0.00310	0.503	0.526
328	781	0.00305	0.868	0.918
333	1110	0.00300	1.204	1.297

Eyring plot

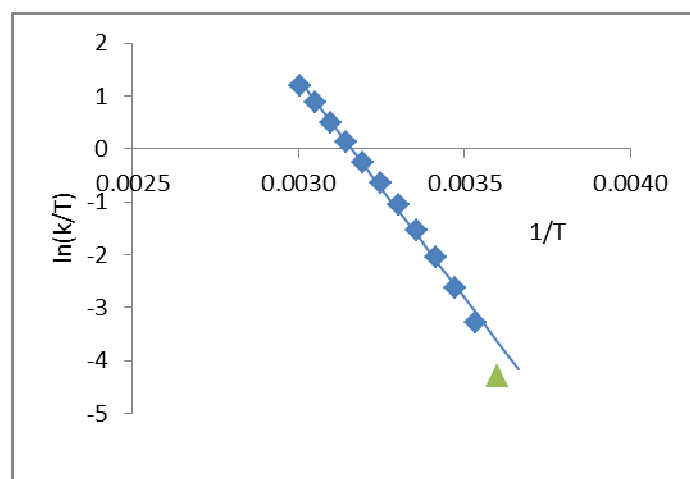


Figure S24. Eyring plot (ln k/T vs 1/T) for (^{Me}BDI)Rh(BD) over the range 273-333 K.

Fit results:

$$\Delta H^\ddagger = 68.9 \pm 1.4 \text{ kJ mol}^{-1} \quad 16.5 \pm 0.3 \text{ kcal mol}^{-1}$$

$$\Delta S^\ddagger = 20.2 \pm 4.5 \text{ J mol}^{-1} \text{ K}^{-1} \quad 4.8 \pm 1.1 \text{ cal mol}^{-1} \text{ K}^{-1}$$

NMR spectra for (^{Me}BDI)Ir(BD)

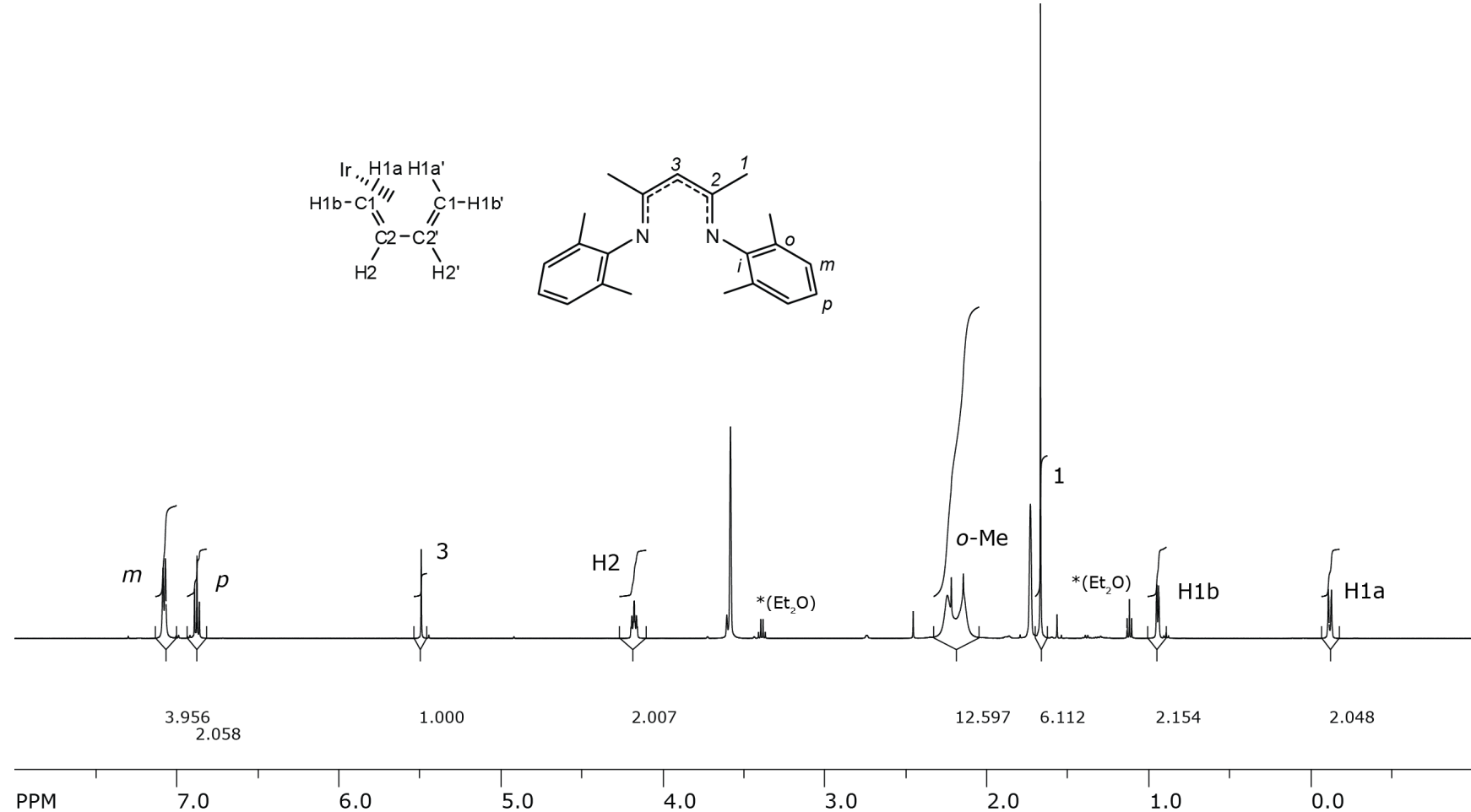


Figure S25. ¹H NMR spectrum of (^{Me}BDI)Ir(BD) (THF-*d*₈, 298K).

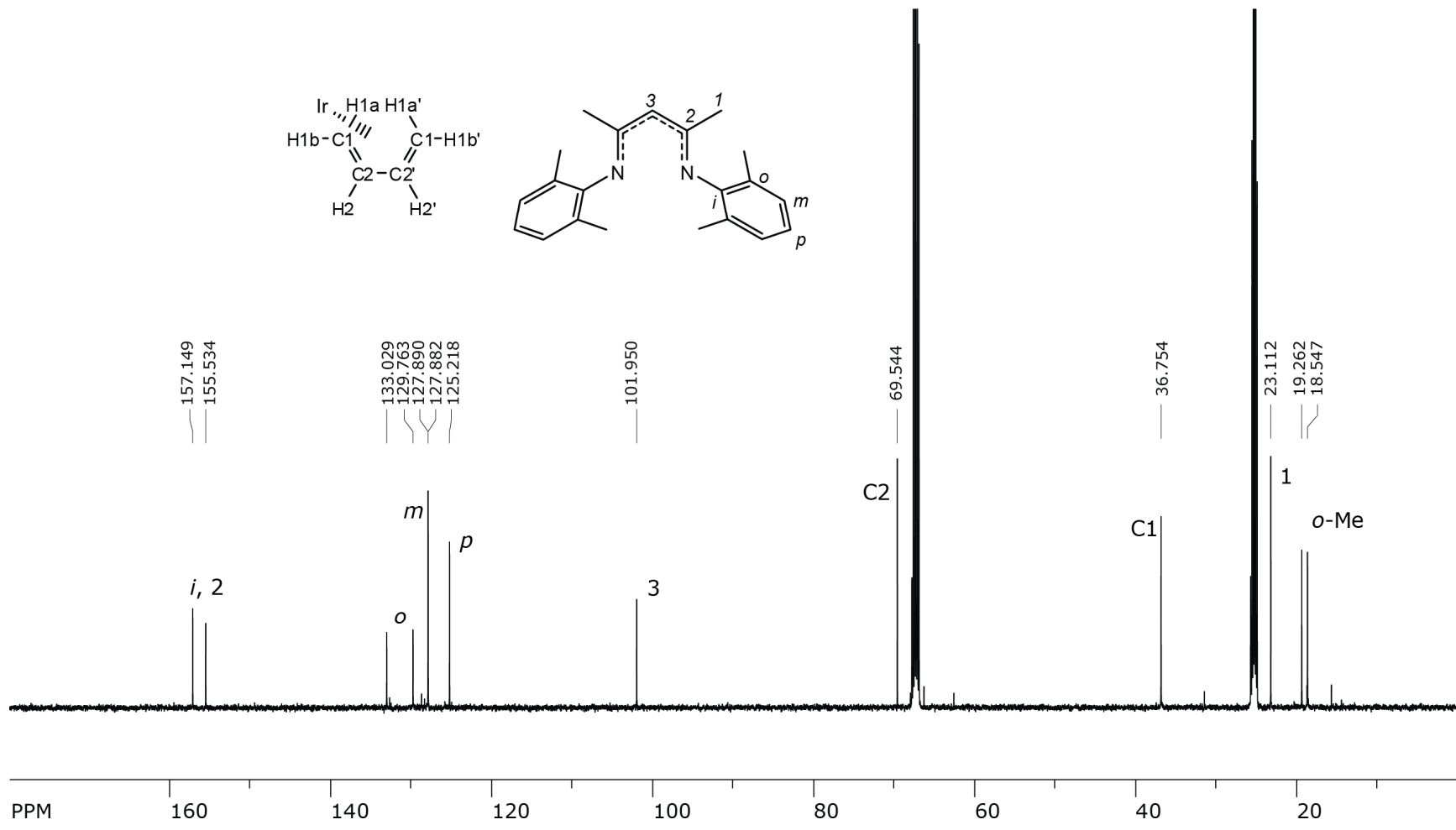


Figure S26. ^{13}C NMR spectrum of $(^{\text{Me}}\text{BDI})\text{Ir}(\text{BD})$ (THF- d_8 , 268K).

Simulation of VT-NMR spectra, (^{Me}BDI)Ir(BD), aryl methyl region.

Table S7. Fitted rate constants for VT-NMR spectra of (^{Me}BDI)Rh(BD).

T (K)	k (mol L ⁻¹)	1/T	ln(k/T)	pred ln(k/T)
263	~0	0.00380		-5.460
268	~0	0.00373		-4.858
273	1.7	0.00366	-5.079	-4.278
278	5.1	0.00360	-3.998	-3.719
283	11.3	0.00353	-3.221	-3.180
288	20.1	0.00347	-2.662	-2.660
293	37.8	0.00341	-2.048	-2.157
298	61.7	0.00336	-1.575	-1.671
303	112	0.00330	-0.995	-1.202
308	175	0.00325	-0.565	-0.747
313	277	0.00319	-0.122	-0.307
318	340	0.00314	0.067	0.119
323	486	0.00310	0.409	0.532
328	628	0.00305	0.650	0.932

Eyring plot

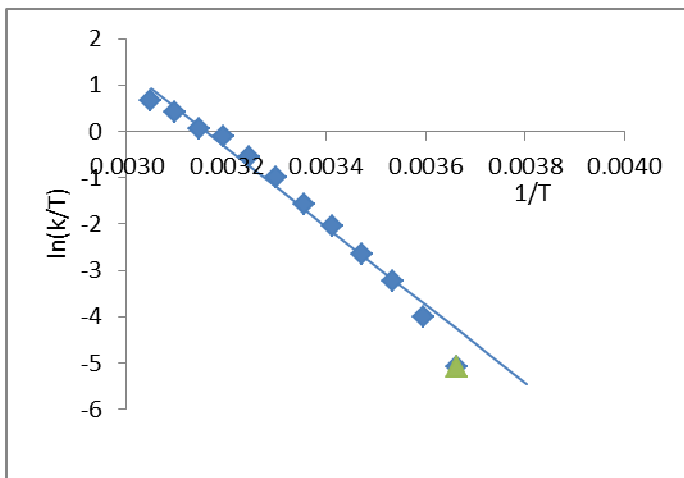


Figure S27. Eyring plot ($\ln k/T$ vs $1/T$) for (^{Me}BDI)Ir(BD) over the range 263–328 K.

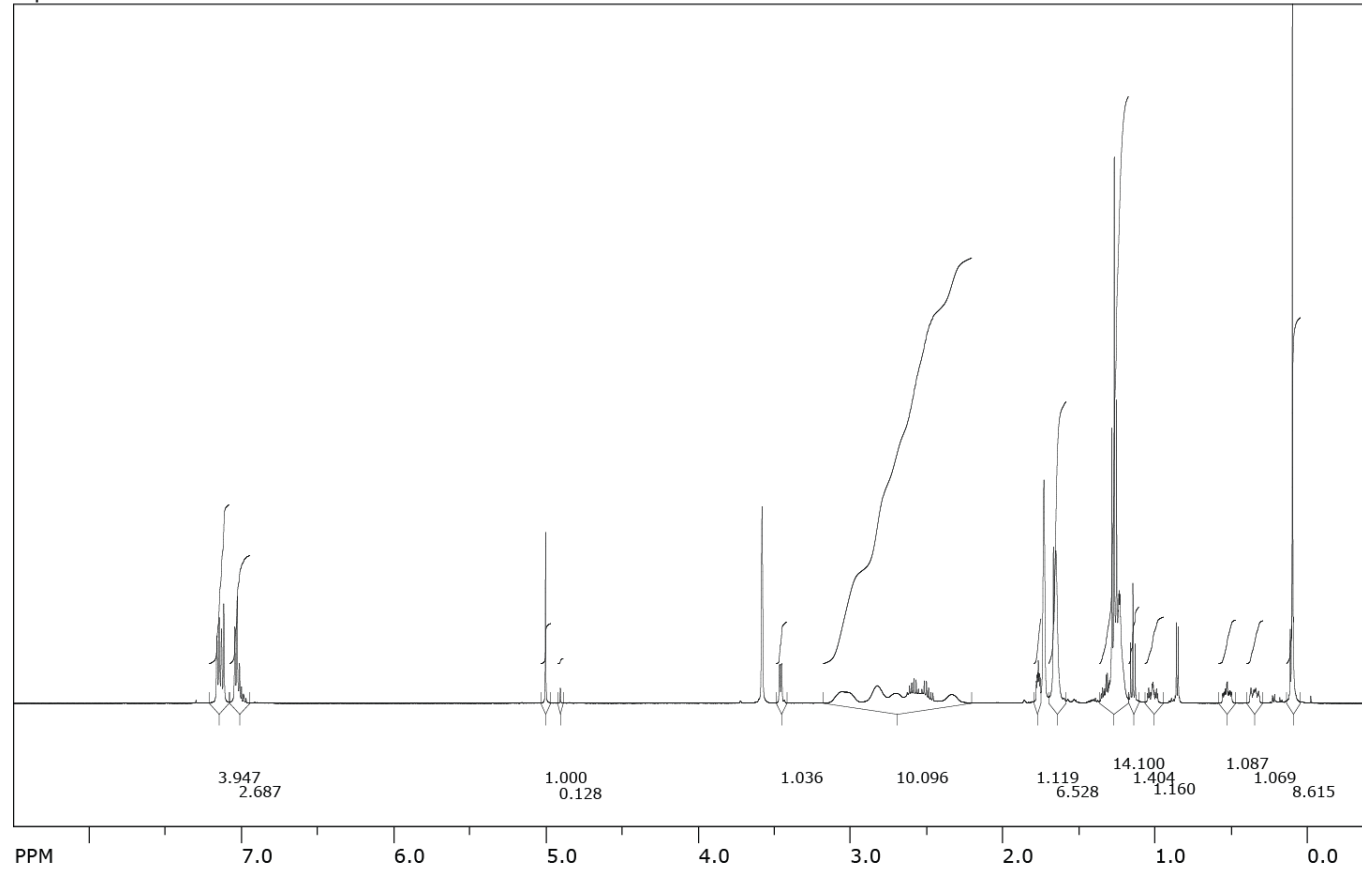
Fit results:

$$\Delta H^\ddagger = 70.5 \pm 2.7 \text{ kJ mol}^{-1} \quad 16.8 \pm 0.6 \text{ kcal mol}^{-1}$$

$$\Delta S^\ddagger = 25.2 \pm 8.9 \text{ J mol}^{-1} \text{ K}^{-1} \quad 6.0 \pm 2.1 \text{ cal mol}^{-1} \text{ K}^{-1}$$

NMR spectra for (^{Et}BDI)Rh(2-TMSO-1,3-CHD)

SpinWorks 4: RSS-1-95 OTMSCHD



file: ...data\RSS-1-95 EtBDIRhOTMSCHD\1\fid expt: <zg30>
transmitter freq.: 500.133089 MHz
time domain size: 65536 points
width: 10000.00 Hz = 19.9947 ppm = 0.152588 Hz/pt
number of scans: 16

freq. of 0 ppm: 500.130020 MHz
processed size: 65536 complex points
LB: 0.300 GF: 0.0000

Figure S28. ¹H NMR spectrum of (^{Et}BDI)Rh(2-TMSO-1,3-CHD) (THF-*d*₈, 298K), overview.

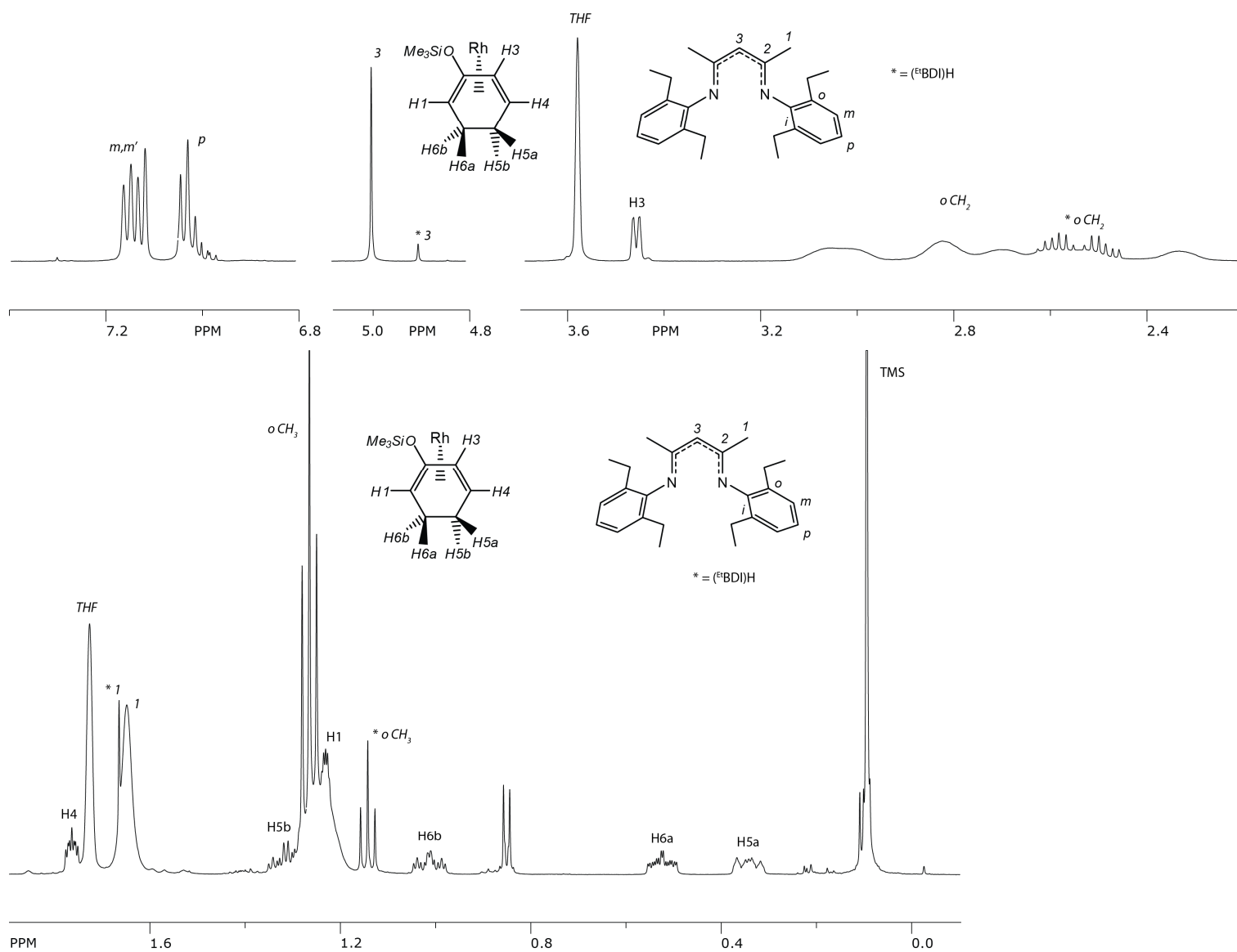
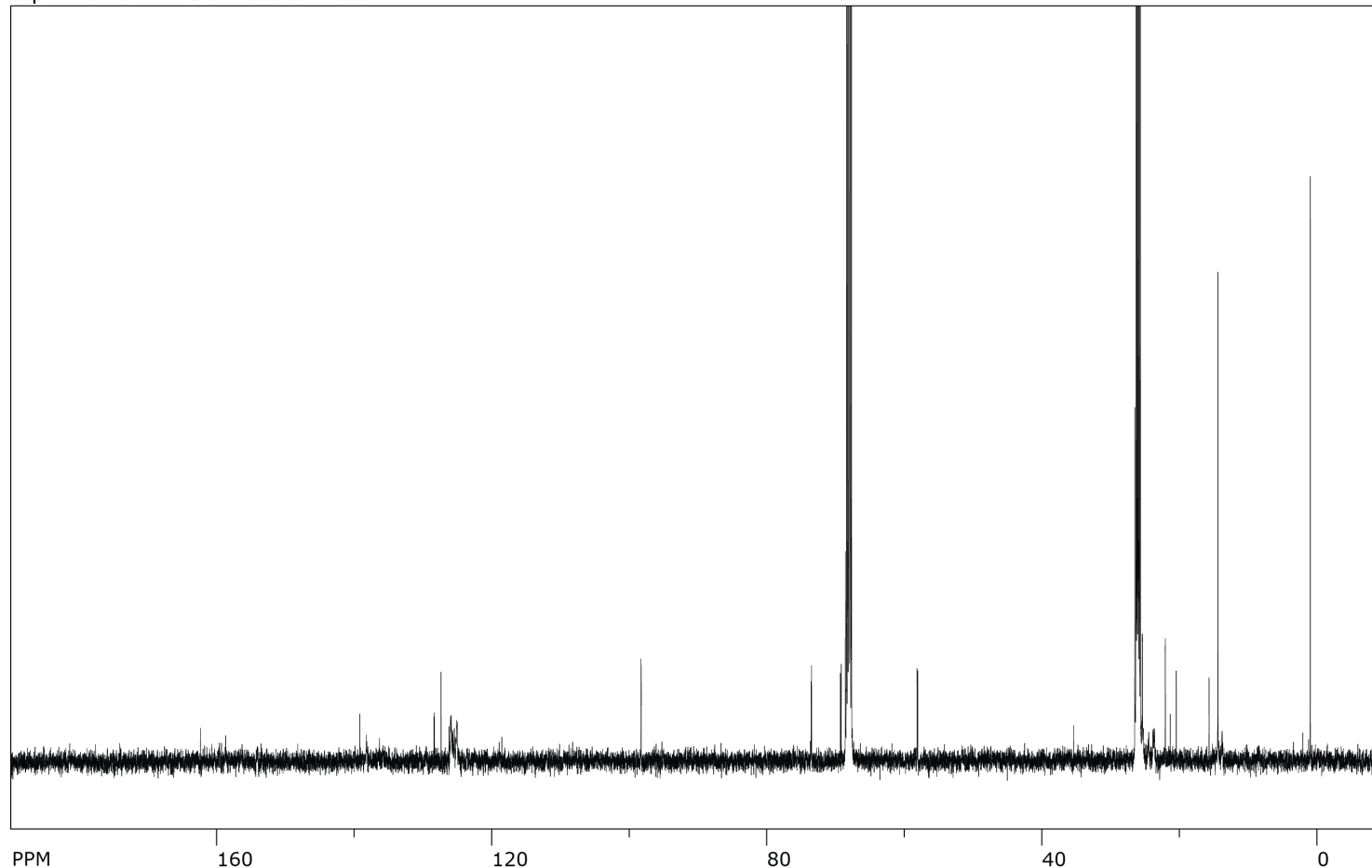


Figure S29. ^1H NMR spectrum of $(^{\text{Et}}\text{BDI})\text{Rh}(2\text{-TMSO-1,3-CHD})$ ($\text{THF-}d_8$, 298K), assignments.

SpinWorks 4: RSS-1-95 OTMSCHD



file: ...data\RSS-1-95 EtBDIRhOTMSCHD\2\fid expt: <zgpg30>
transmitter freq.: 125.770364 MHz
time domain size: 65536 points
width: 29761.91 Hz = 236.6369 ppm = 0.454131 Hz/pt
number of scans: 1024

freq. of 0 ppm: 125.757587 MHz
processed size: 32768 complex points
LB: 1.000 GF: 0.0000

Figure S30. ¹³C NMR spectrum of (^{Et}BDI)Rh(2-TMSO-1,3-CHD) (THF-*d*₈, 298K), overview.

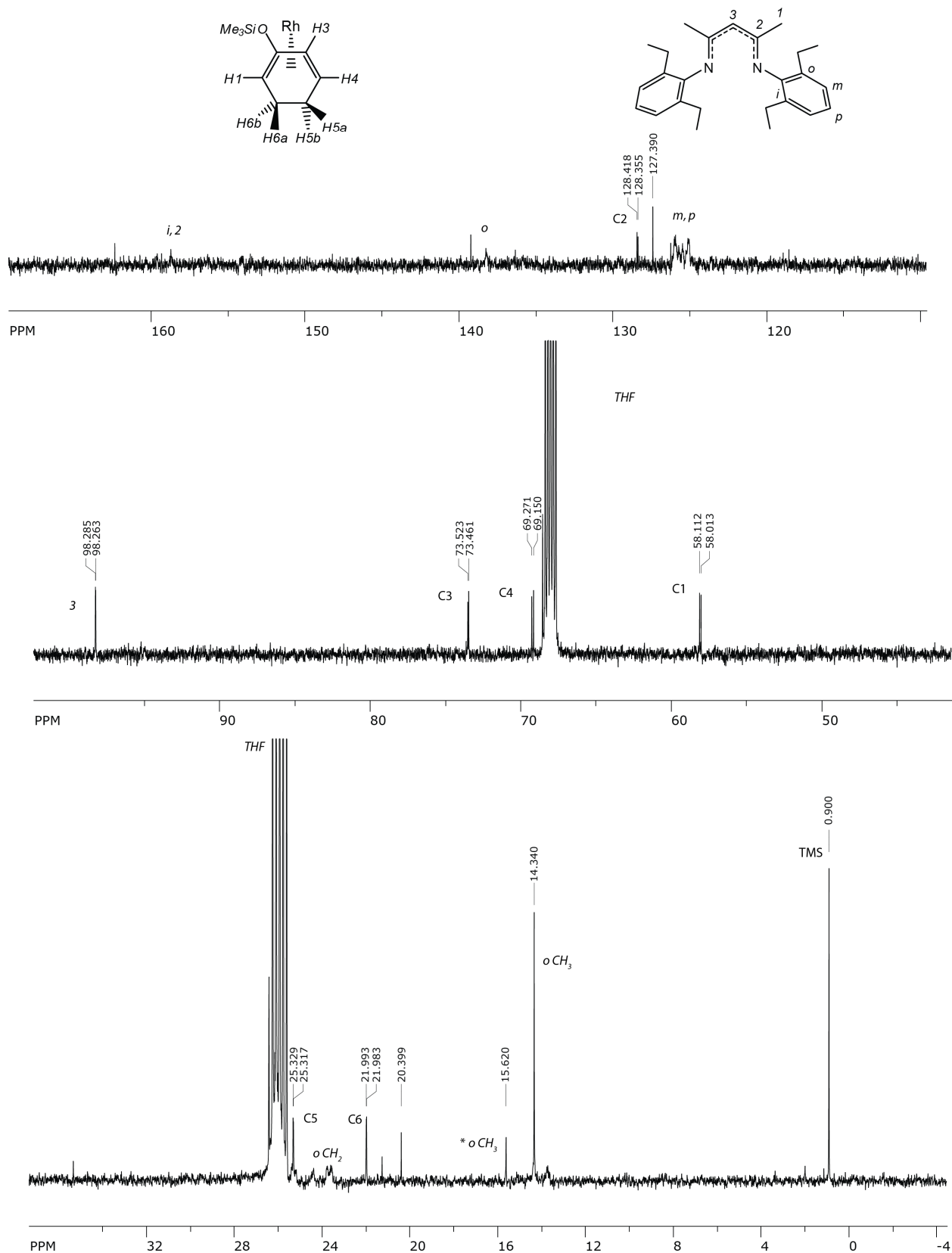


Figure S31. ^{13}C NMR spectrum of $(\text{Et}^{\text{t}}\text{BDI})\text{Rh}(2\text{-TMSO-1,3-CHD})$ ($\text{THF-}d_8$, 298K), assignments.

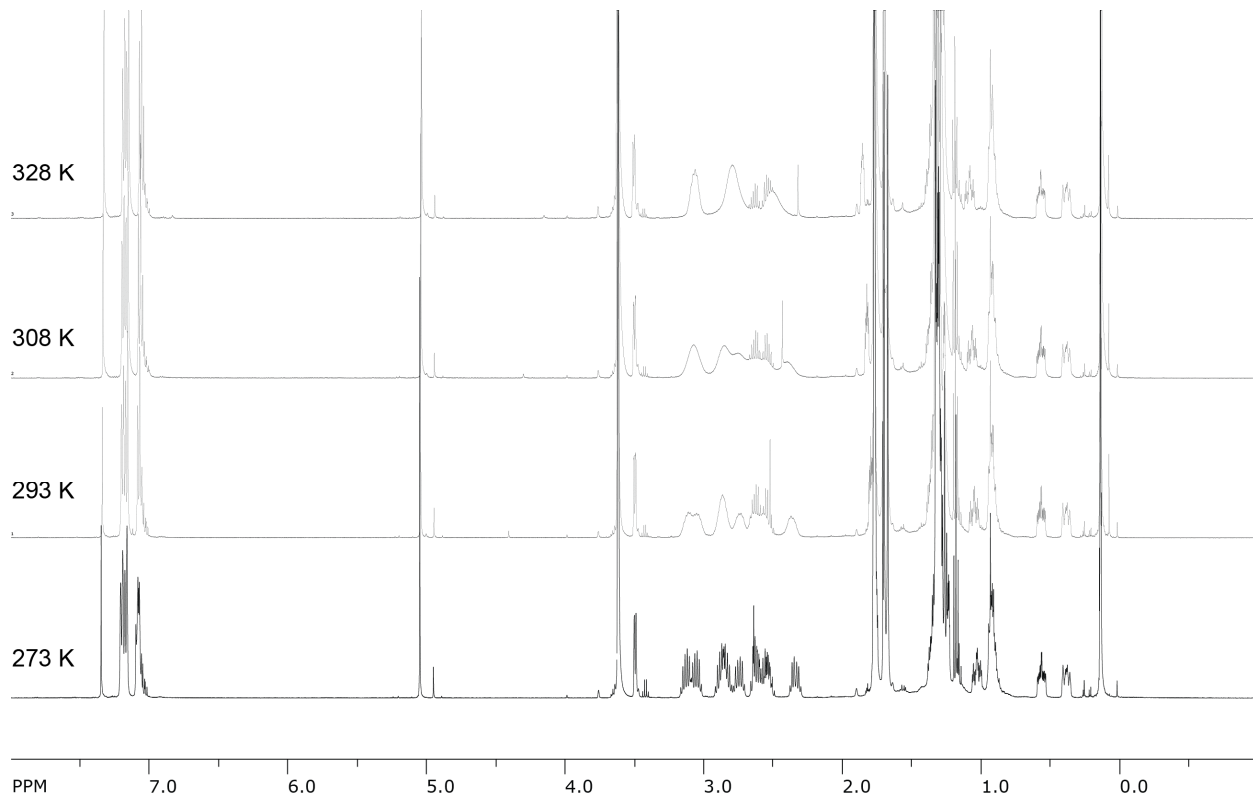
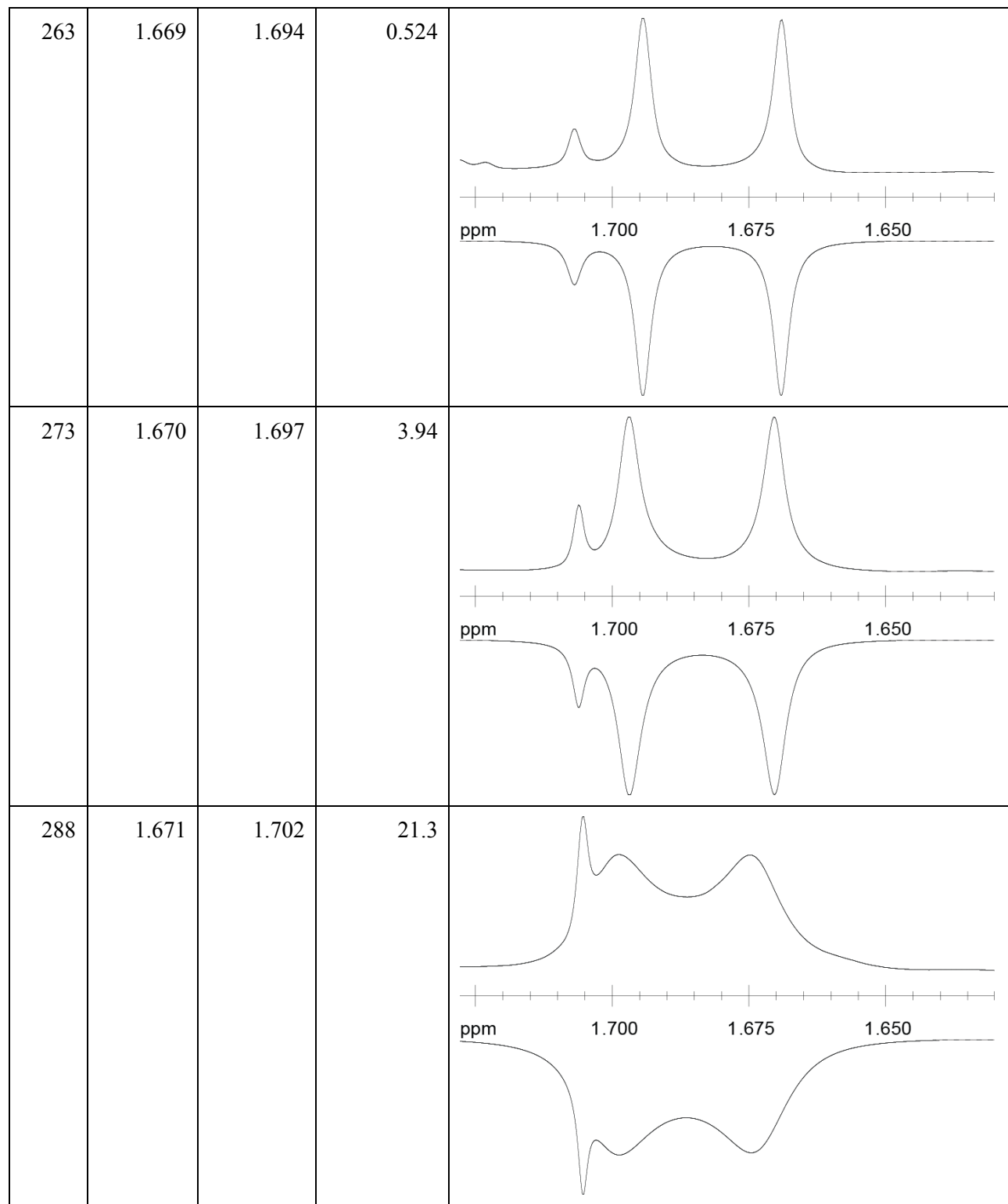


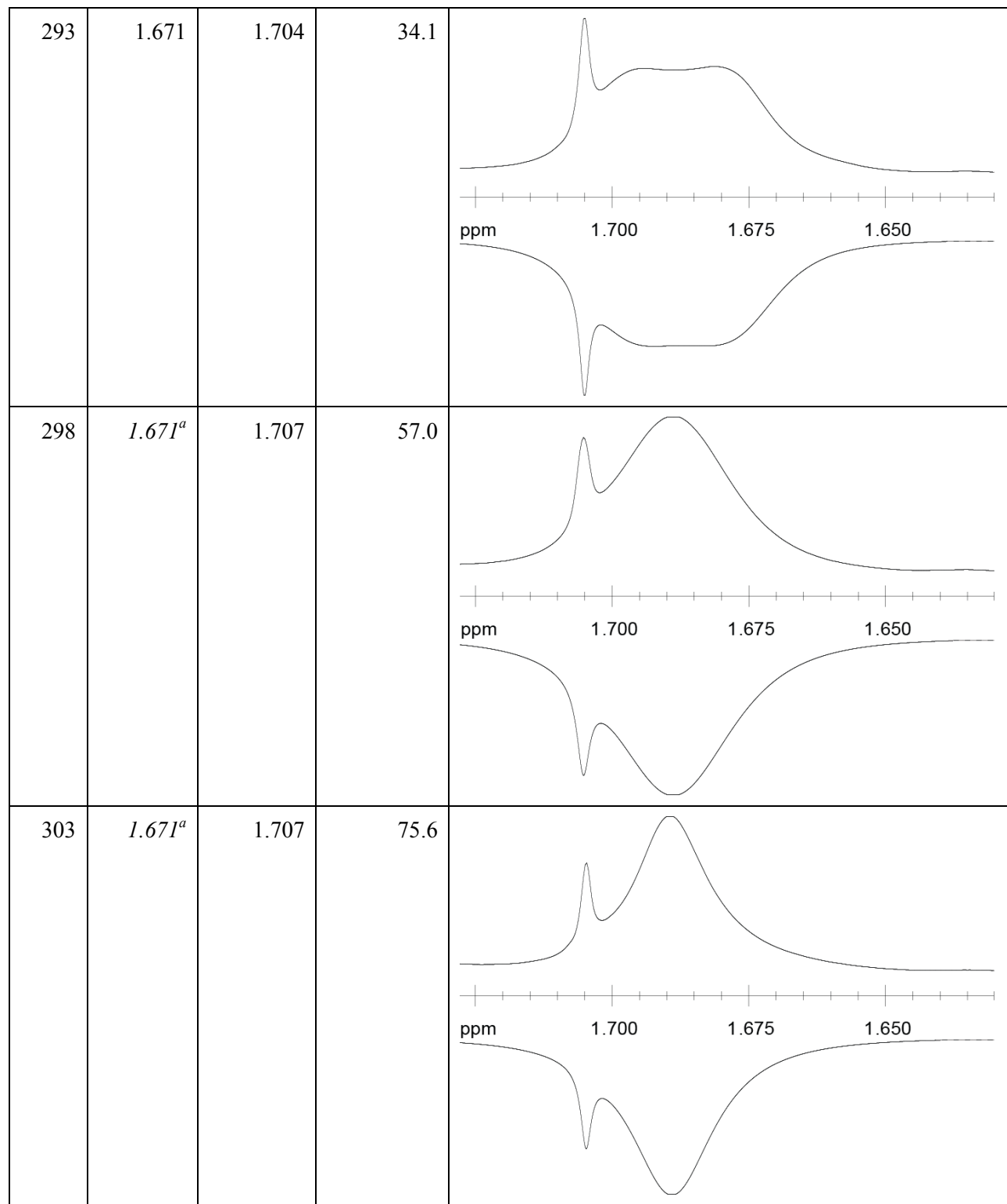
Figure S32. Selected ¹H VT-NMR spectra for (^{Et}BDI)Rh(2-TMSO-1,3-CHD) (THF-*d*₈).

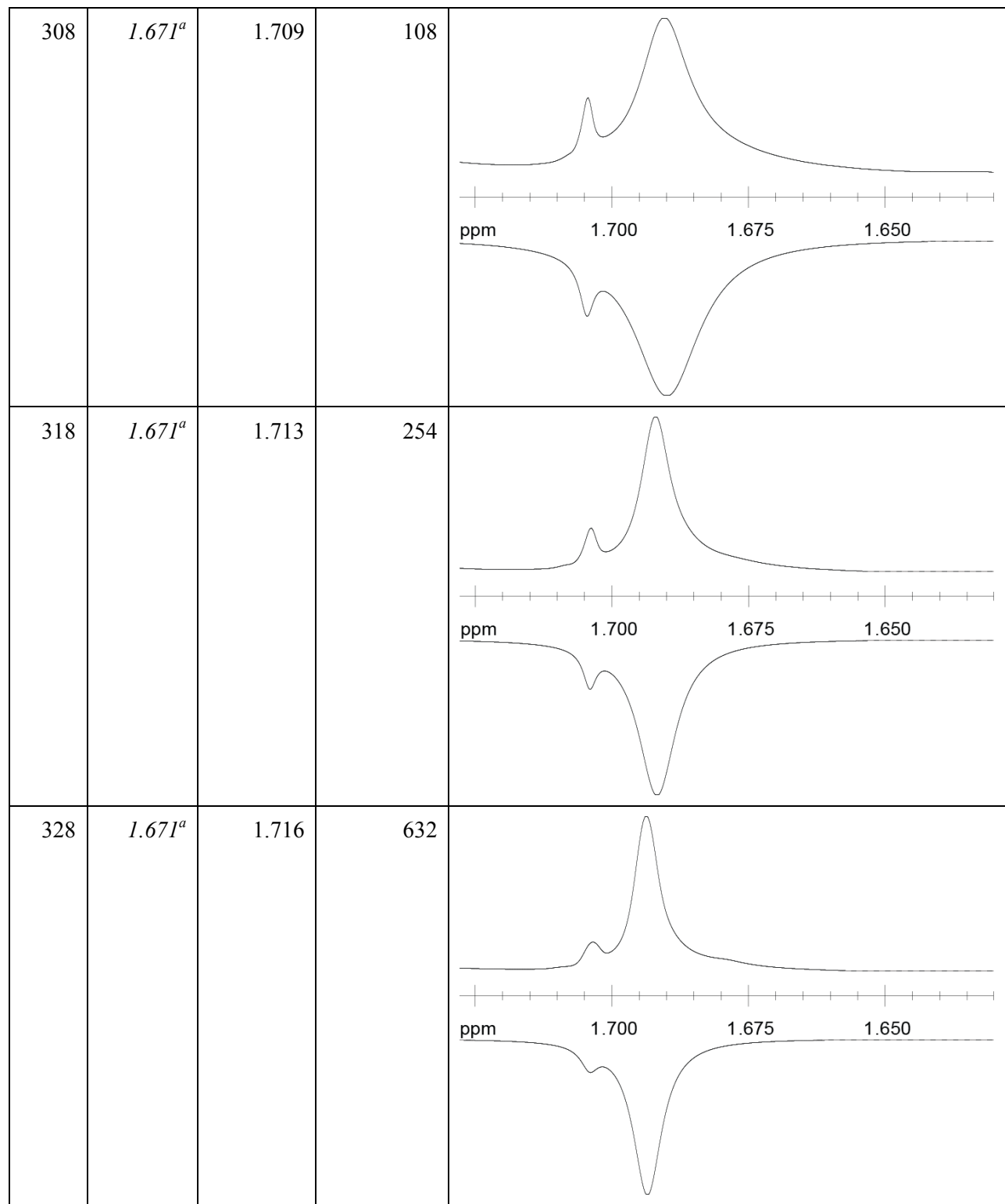
Simulation of VT-NMR spectra, (^{Et}BDI)Rh(2-TMSO-1,3-CHD), imine methyl region.

Table S8. Chemical shifts of imine methyl groups, fitted rate constants, and fitted spectrum traces for VT-NMR spectra of (^{Et}BDI)Rh(2-TMSO-1,3-CHD).

<i>T</i> (K)	δ_1 (ppm)	δ_2 (ppm)	<i>k</i> (mol L ⁻¹)	Fitted spectrum ^b
243	1.665	1.688	~0	
253	1.667	1.691	~0	







^a δ_2 fixed at lower-temperature value for these lineshape fits. ^b Peak near 1.71 ppm is free (^{Et}BDI)H, fitted concentrations 5 mol%.

Eyring plot

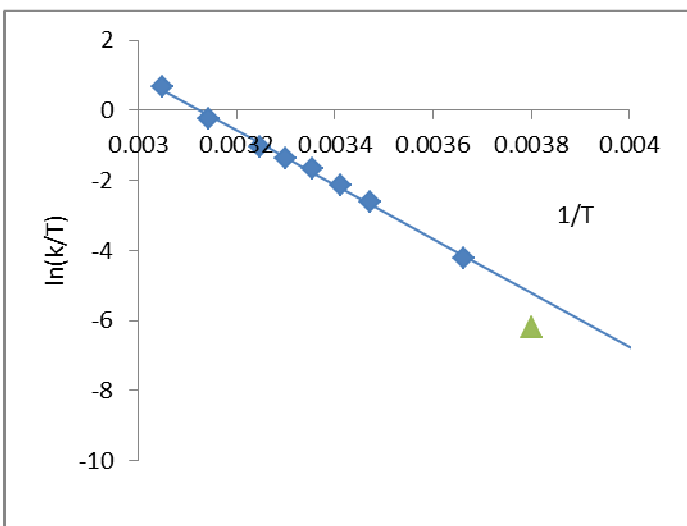


Figure S33. Eyring plot ($\ln k/T$ vs $1/T$) for (^{Et}BDI)Rh(2-TMSO-1,3-CHD) over the range 273-328 K.

Fit results:

$$\Delta H^\ddagger = 64.3 \pm 1.6 \text{ kJ mol}^{-1} \quad 15.4 \pm 0.4 \text{ kcal mol}^{-1}$$

$$\Delta S^\ddagger = 3.5 \pm 5.3 \text{ J mol}^{-1} \text{ K}^{-1} \quad 0.8 \pm 1.3 \text{ cal mol}^{-1} \text{ K}^{-1}$$

Calculated b-p energies

Table S9. Calculated b-p energies, thermal and dispersion corrections, and rotation activation parameters.^a

Name	b-p/tzvp			b-p/tzvpp			H	S	G	H _{rel}	S _{rel}	G _{rel}
	H _{corr}	TS _{corr}	Dispersion	E _{elec}	<S ² >	a.u.						
MeBDI_Rh_Bd (3)	0.51376	0.09208	-0.09416	-1192.03157		-1191.61197	0.000309	-1191.70404	0.00	0.00	0.00	0.00
MeBDI_Rh_Bd_rotTS	0.51173	0.09008	-0.09148	-1192.01114		-1191.59089	0.000302	-1191.68098	13.23	-4.19	14.48	
MeBDI_Rh_Bd_triplet ^b	0.51204	0.09419	-0.09204	-1191.98668	2.01	-1191.56667	0.000316	-1191.66086	28.42	4.45	27.10	
MeBDI_Rh_Bd_rotTS_triplet ^b	0.51053	0.09049	-0.09332	-1191.96078	2.01	-1191.54358	0.000304	-1191.63407	42.92	-3.34	43.91	

^a Thermal corrections calculated from vibrational analysis at b-p/TZVP optimized geometries, 298 K, 1 bar, gas phase. Total electronic energies and DFT-D3 dispersion corrections calculated using b-p/TZVPP at TZVP geometries. H = E_{elec}+Dispersion+H_{corr}; G = E_{elec}+Dispersion+H_{corr}-S_{corr}. ^b The preferred BD orientations for singlet and triplet are opposite, so the geometry of the singlet rotation TS resembles the triplet minimum and vice versa.

Name	TPSSh/tzvp			TPSSh/tzvpp			$\langle S^2 \rangle$	H	S	G	H _{rel}	S _{rel}	G _{rel}
	H _{corr} a.u.	TS _{corr} a.u.	Dispersion a.u.	E _{elec} a.u.	a.u.	a.u./K							
EtBDI_Ir	0.55206	0.09661	-0.06464	-1186.84986	-1186.36244	0.000324	-1186.45905						
EtBDI_Ir_CO2	0.57473	0.10380	-0.07678	-1413.76916	-1413.27120	0.000348	-1413.37500						
EtBDI_Ir_CO2_rotTS	0.57252	0.10413	-0.07499	-1413.71159	-1413.21405	0.000349	-1413.31818	35.86	0.69	35.65			
EtBDI_Ir_Eth2	0.66878	0.10246	-0.08912	-1344.23037	-1343.65071	0.000344	-1343.75317						
EtBDI_Ir_Eth2_rotTS	0.66634	0.10141	-0.08787	-1344.19445	-1343.61599	0.000340	-1343.71739	21.79	-2.22	22.45			
EtBDI_Ir_COD	0.74384	0.10645	-0.10297	-1499.15145	-1498.51059	0.000357	-1498.61704						
EtBDI_Ir_COD_rotTS	0.74096	0.10739	-0.10342	-1499.11100	-1498.47347	0.000360	-1498.58086	23.29	1.98	22.70			
EtBDI_Ir_Bd	0.64562	0.10270	-0.08502	-1343.03510	-1342.47450	0.000345	-1342.57720						
EtBDI_Ir_Bd_rotTS	0.64376	0.10101	-0.08354	-1343.01202	-1342.45180	0.000339	-1342.55282	14.24	-3.56	15.30			

^a Thermal corrections calculated from vibrational analysis at TPSSh/TZVP optimized geometries, 298 K, 1 bar, gas phase. Total electronic energies and DFT-D3 dispersion corrections calculated using TPSSh/TZVPP at TZVP geometries. H = E_{elec}+Dispersion+H_{corr}; G = E_{elec}+Dispersion+H_{corr}-S_{corr}. ^b The preferred BD orientations for singlet and triplet are opposite, so the geometry of the singlet rotation TS resembles the triplet minimum and vice versa.